



Ionic and carbonaceous compositions of PM_{10} , $PM_{2.5}$ and $PM_{1.0}$ at Gosan ABC Superstation and their ratios as source signature

S. Lim^{1,*}, M. Lee¹, G. Lee², S. Kim³, S. Yoon³, and K. Kang⁴

¹Dept. of Earth and Environmental Sciences, Korea University, Seoul, South Korea

²Dept. of Environmental Science, Hankuk University of Foreign Studies, Yongin, South Korea

³School of Earth and Environmental Sciences, Seoul National University, Seoul, South Korea

⁴College of Ocean Science, Jeju National University, Jeju, South Korea

* now at: Laboratoire de Glaciologie et Géophysique de l'Environnement (LGGE), CNRS/University of Grenoble, Grenoble, France

Correspondence to: M. Lee (meehye@korea.ac.kr)

Received: 26 April 2011 – Published in Atmos. Chem. Phys. Discuss.: 19 July 2011

Revised: 30 January 2012 – Accepted: 2 February 2012 – Published: 21 February 2012

Abstract. $PM_{1.0}$, $PM_{2.5}$, and PM_{10} were sampled at Gosan ABC Superstation on Jeju Island from August 2007 to September 2008. The carbonaceous aerosols were quantified with the thermal/optical reflectance (TOR) method, which produced five organic carbon (OC) fractions, OC1, OC2, OC3, OC4, and pyrolyzed organic carbon (OP), and three elemental carbon (EC) fractions, EC1, EC2, and EC3. The mean mass concentrations of $PM_{1.0}$, $PM_{2.5}$, and PM_{10} were $13.7 \mu\text{g m}^{-3}$, $17.2 \mu\text{g m}^{-3}$, and $28.4 \mu\text{g m}^{-3}$, respectively. The averaged mass fractions of OC and EC were 23.0% and 10.4% for $PM_{1.0}$, 22.9% and 9.8% for $PM_{2.5}$, and 16.4% and 6.0% for PM_{10} . Among the OC and EC sub-components, OC2 and EC2+3 were enriched in the fine mode, but OC3 and OC4 in the coarse mode. The filter-based $PM_{1.0}$ EC agreed well with black carbon (BC) measured by an Aethalometer, and PM_{10} EC was higher than BC, implying less light absorption by larger particles. EC was well correlated with sulfate, resulting in good relationships of sulfate with both aerosol scattering coefficient measured by Nephelometer and BC concentration. Our measurements of EC confirmed the definition of EC1 as char-EC emitted from smoldering combustion and EC2+3 as soot-EC generated from higher-temperature combustion such as motor vehicle exhaust and coal combustion (Han et al., 2010). In particular, EC1 was strongly correlated with potassium, a traditional biomass burning indicator, except during the summer, when the ratio of EC1 to EC2+3 was the lowest. We also found the ratios of major chemical species to be a useful tool to constrain the main sources of aerosols, by which the five air masses were well distinguished: Siberia, Beijing,

Shanghai, Yellow Sea, and East Sea types. Except Siberian air, the continental background of the study region, Beijing plumes showed the highest EC1 (and OP) to sulfate ratio, which implies that this air mass had the highest net warming by aerosols of the four air masses. Shanghai-type air, which was heavily influenced by southern China, showed the highest sulfate enhancement. The highest EC2+3/EC1 ratio was found in aged East Sea air, demonstrating a significant influence of motor vehicle emissions from South Korea and Japan and less influence from industrial regions of China. The high ratio results from the longer residence time and less sensitivity to wet scavenging of EC2+3 compared to EC1, indicating that soot-EC could have greater consequence in regional-scale warming.

1 Introduction

Atmospheric aerosols play an important role in climate change by influencing the global radiation balance both directly and indirectly. The direct effect is the mechanism by which aerosols scatter and absorb shortwave and longwave radiation, thereby altering the radiative balance of the Earth-atmosphere system (IPCC, 2007). The relative importance of these processes depends on the chemical composition and size distribution of aerosols (Ramachandran et al., 2009). Aerosols also cause a negative radiative forcing indirectly through changes in cloud properties. This indirect effect includes the role of aerosols in modifying cloud droplet

number concentration and cloud lifetime (IPCC, 2007; Haywood and Boucher, 2000).

Because the chemical composition and size distribution of aerosols are important in quantifying their radiative effects (Brasseur et al., 1999; Ramanathan et al., 2001; Buzorius et al., 2004), knowledge of the chemical composition of atmospheric aerosols of a given size is required to assess their impact on the environment. Aerosols are often classified into submicron and supermicron particles; the former are of particular concern to public health and climate change because they mainly originate from anthropogenic sources and interact more efficiently with sunlight. Anthropogenic sources contribute almost as much as natural sources to the global aerosol optical depth (AOD) (Hansen et al., 1997; Robertson et al., 2001).

Anthropogenic aerosols are typically composed of various inorganic and organic species (IPCC, 2007), among which sulfate, nitrate, and carbonaceous aerosols including black carbon (BC) and organic carbon (OC) are of major interest due to their atmospheric abundances. In particular, carbonaceous aerosols are major contributors to fine aerosols smaller than 1 µm and typically constitute a significant, sometimes dominant, fraction of the total fine particle mass of submicron particles (Gray et al., 1986; Shah et al., 1986; Andrews et al., 2000; Yang et al., 2005). They are composed of light-absorbing carbon as well as light-scattering carbon. The radiative forcing at the top of the atmosphere is found to change sign from negative to positive when carbonaceous aerosols are abundant over highly reflecting surfaces such as land and snow, which results in higher atmospheric heating (Ramanathan and Carmichael, 2008; Ramachandran et al., 2009).

These carbonaceous aerosols are mainly divided into two categories: elemental carbon (EC), often called BC or soot, and OC. Especially for EC, there are various definitions and analytical methods to quantify its atmospheric concentration (Andreae and Gelencsér, 2006; Han et al., 2010). EC is usually referred to a near-elemental soot-carbon-like composition and to the fraction of carbon that is oxidized in combustion analysis above a certain temperature threshold. Soot carbon may be defined as aggregates of spherules made of grapheme layers, consisting almost purely of carbon, with minor amounts of bound heteroelements, especially hydrogen and oxygen, whereas BC is referred to a black, blackish or brown substance formed by combustion, present in the atmosphere as fine particles. BC generally implies to have optical properties and composition similar to soot carbon. While EC is usually determined by thermal methods based on its chemical properties, BC is measured using its optical properties. Therefore, BC and EC may show slightly different concentrations due to their different quantification techniques. EC enters the atmosphere exclusively as a primary (i.e. direct particulate) emission originating nearly completely from pyrolysis during incomplete combustion, mainly of biomass and fossil fuel (Nunes and

Pio, 1993; Bond et al., 2007). Because EC is optically absorptive and highly polyaromatic, it has recently been a subject of interest in many studies encompassing local to global scales. In particular, EC (or BC) could be the next most important contributor to global warming, in terms of direct forcing, after CO₂ (Jacobson, 2001; Ramanathan and Xu, 2010). The surface forcing is about 2–3 times larger than the forcing at the top of the atmosphere for absorbing aerosols such as EC, producing a large atmospheric warming (Ramanathan and Carmichael, 2008).

On the other hand, OC is commonly considered as the non-absorptive fraction of the carbonaceous aerosol. It has more molecular forms and a lower molecular weight than EC. OC is produced from both direct emission and gaseous precursors by atmospheric oxidation or oligomerization (Jacobson et al., 2000; Kanakidou et al., 2005; Tsigaridis et al., 2006). The main primary source of OC is combustion along with EC emissions and biogenic emissions. In addition, OC is produced from oxidation of precursor gases in the atmosphere, constituting what is called secondary organic aerosol (SOA). A considerable proportion of organic aerosols is hygroscopic, thereby serving as cloud condensation nuclei (CCN) along with sulfate aerosols. On the other hand, EC particles are hydrophobic when they are emitted, but the sulfates or water soluble organic compounds (WSOC) that become attached to EC particles can change them from hydrophobic to hydrophilic, eventually making them efficient CCN (Decesari et al., 2002; Persiantseva et al., 2004; Petzold et al., 2005). When EC was coated with reflecting compounds like OC, the absorption by EC was found to increase at least by a factor of 1.5 (Bond et al., 2006). In addition, carbonaceous aerosols, when mixed with atmospheric dust, have the potential to influence the atmospheric chemistry of several trace gases such as NO₂, O₃, and SO₂ (Dentener et al., 1996).

Although the definition and measurement techniques for atmospheric EC or BC have long been subjects of scientific controversy, the recent discovery of light-absorbing carbon that is not black but brown (or yellowish) makes it imperative to reassess and redefine the components that make up light-absorbing carbonaceous matter in the atmosphere (Andreae and Gelencsér, 2006). There has been growing evidence for the contribution of brown carbon to light absorption in atmospheric aerosols from chemical aerosol measurements and laboratory studies (Mukai and Ambe, 1986; Havers et al., 1998; Hoffer et al., 2006; Alexander et al., 2008; Park et al., 2010).

Aerosols are more concentrated in the source regions and exhibit strong spatial and temporal variations. Furthermore, they have an impact on global climate because their radiative influence can be transported due to changes in the mean atmospheric circulation patterns (Ramachandran et al., 2009). Therefore, finding a source and a source region of major components of aerosols, such as carbonaceous species, sulfate, and nitrate, is crucial for the assessment of their

radiative effect. In particular, Asia is the main source of global anthropogenic aerosol emission. At present, anthropogenic emissions of gaseous pollutants in Asia are larger than those in Europe and North America and will continue to increase in the future (Akimoto, 2003). An emission inventory study in Asia suggests that 30–60% of the total emission of aerosol gaseous precursors and primary BC and OC are emitted in China (Streets et al., 2003), in particular, ~41% of submicron BC. The recently documented linear increase of primary BC and OC between 1850 and 2000 highlights the importance of continuous measurements of carbonaceous particles (Bond et al., 2007). Additionally, the frequent presence of desert dust makes the East Asian atmosphere more complex because of both scattering of sunlight and absorption of radiation (Huebert et al., 2003).

In recent decades, carbonaceous aerosols, both EC and OC, have been measured in many regions of Northeast Asia, including South Korea, China, and Japan (Ohta et al., 1998; Kim et al., 2000; He et al., 2001; Park et al., 2001; Ye et al., 2003; Cao et al., 2005; Hagler et al., 2006; Lee et al., 2007, 2008; Shen et al., 2007; Zhang et al., 2007; Moon et al., 2008; Aggarwal and Kawamura, 2009; Lee et al., 2009). The areas covered have included urban areas (He et al., 2001; Park et al., 2001; Ye et al., 2003; Zhang et al., 2007; Lee et al., 2009), developing regions (Hagler et al., 2006), and sandlands (Cao et al., 2005; Shen et al., 2007). Most of these studies focused on PM_{2.5} through a year (He et al., 2001; Ye et al., 2003) and PM_{2.5} or PM₁₀ during a specific season, such as spring (Lee et al., 2007; Shen et al., 2007), spring and early summer (Aggarwal and Kawamura, 2009), fall and winter (Cao et al., 2005), or winter (Zhang et al., 2007). There have been few year-round studies of both fine and coarse aerosols, particularly at a site where it is feasible to monitor long-range transport and the atmospheric processes involving air pollutants emitted from the Asian continent. This limitation hinders the full characterization of carbonaceous aerosols in Northeast Asia.

In the present study, we measured soluble ionic species, OC, and EC in PM_{1.0}, PM_{2.5}, and PM₁₀ at Gosan ABC Superstation on Jeju Island throughout the year from August 2007 to September 2008. The main objective was three-fold: (1) to better understand the variability of major PM components, particularly OC and EC, of both fine and coarse aerosols; (2) to identify the sources of these components; and finally (3) to examine the relationships between chemical compositions and optical properties.

2 Measurement

PM_{1.0}, PM_{2.5}, and PM₁₀ were measured at Gosan ABC Superstation on Jeju Island during August 2007–September 2008. Gosan station (33.17° N, 126.10° E, 70 m a.s.l., Fig. 1) served as a base for the ACE-Asia experiment in 2001 and was designated as one of the ABC Su-

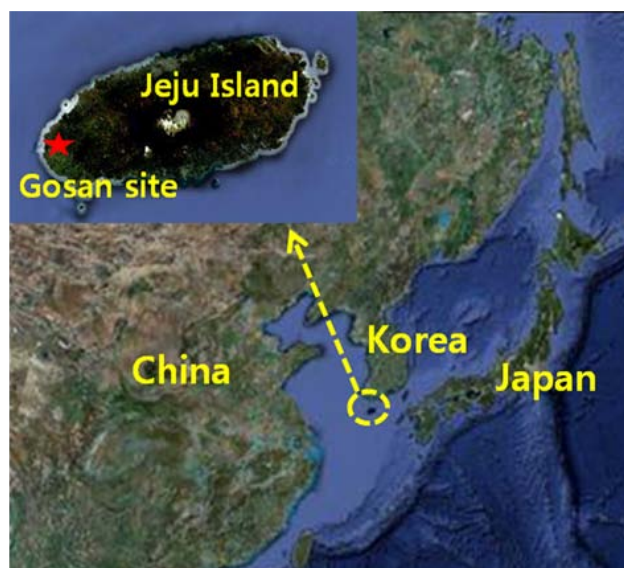


Fig. 1. Map showing Gosan ABC superstation (33.17° N, 126.10° E, 70 m a.s.l.) from Google mapmaker (<http://www.google.com/mapmaker>). The station is located on the west coast of Jeju Island, South Korea.

perstations (Lee et al., 2007). It has been considered to be an ideal location to monitor Asian outflows and assess their impact on air quality over the northern Pacific (Carmichael et al., 1996, 1997; Chen et al., 1997).

In the present study, the concentrations of water-soluble inorganic ions, EC, OC, and mass in PM_{1.0}, PM_{2.5}, and PM₁₀ were measured for about one year. Ambient air was collected through PM_{1.0}, PM_{2.5}, and PM₁₀ sharp-cut cyclone coated with Teflon (URG, USA) at 16.7 LPM, and cumulative flow was measured with a dry gas-meter. These low-volume samplers were installed at the top of a 10-m tower. Particles were collected on pre-weighed 37-mm Teflon filters for mass and ion analysis, and on pre-heated 37-mm quartz-fiber filters (Pall corp., USA) for carbon analysis.

Sampling was conducted usually once every six days. It started at 09:00 LST and lasted for 24 h. There was less number of samples collected during summer and winter monsoon periods because of rain, snow, or strong wind. With additional samples during particular events such as Asian dust and pollution plumes, a total of 41 sets of samples were taken for this study (Table 1).

Eight species of water-soluble ions, which included SO₄²⁻, NO₃⁻, Cl⁻, NH₄⁺, K⁺, Na⁺, Ca²⁺, and Mg²⁺, were determined by ion chromatography (Dionex 4500, Dionex, USA). More details on this method of analysis can be found in Lim (2009). EC, OC, and TC were analyzed at the Desert Research Institute (Reno, NV, USA) following the Interagency Monitoring of Protected Visual Environments (IMPROVE) thermal/optical reflectance protocol. Thermal/optical methods assume EC is a low-volatility carbon fraction that is not

Table 1. The number of sample sets of PM₁₀, PM_{2.5}, and PM_{1.0} taken from August 2007 to September 2008.

Year	2007				2008								total
	Month	Aug	Oct	Nov	Dec	Jan	Feb	Mar	Apr	May	Jun	Aug	
No.	1	5	4	2	5	3	4	8	4	1	2	2	41

Table 2. Averaged concentrations of mass and major compositions of PM_{1.0}, PM_{2.5}, and PM₁₀.

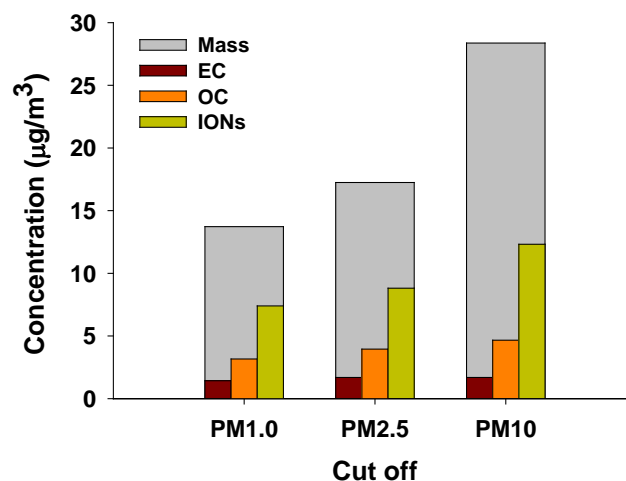
	PM _{1.0}	PM _{2.5}	PM ₁₀
Mass	13.7 ± 7.7	17.2 ± 8.9	28.4 ± 14.1
NO ₃ ⁻	0.7 ± 0.8	1.2 ± 1.1	2.4 ± 1.7
SO ₄ ²⁻	4.6 ± 3.0	5.4 ± 3.6	5.6 ± 3.4
NH ₄ ⁺	1.4 ± 0.7	1.5 ± 0.7	1.6 ± 0.7
OC ^a	3.2 ± 1.8	4.0 ± 2.5	4.7 ± 2.5
OC1	0.2 ± 0.1	0.2 ± 0.1	0.2 ± 0.1
OC2	0.8 ± 0.4	1.0 ± 0.5	1.0 ± 0.5
OC3	0.8 ± 0.4	0.9 ± 0.6	1.3 ± 0.7
OC4	0.5 ± 0.3	0.71 ± 0.6	0.9 ± 0.6
OP	0.9 ± 0.7	1.2 ± 0.8	1.2 ± 0.8
EC ^a	1.4 ± 0.8	1.7 ± 1.3	1.7 ± 1.2
EC1	1.0 ± 0.7	1.3 ± 1.2	1.4 ± 1.0
EC2+3 ^b	0.5 ± 0.2	0.4 ± 0.2	0.3 ± 0.2

All concentrations are given as mean ± standard deviation in μg m⁻³.

^a OC is the sum of OC1, OC2, OC3, OC4, and OP, and EC is the sum of EC1, EC2, and EC3. See the measurement section for the definition of each sub-component. OC1, OC2, OC3, and OC4 are fractions of OC liberated at different temperatures: 120 °C, 250 °C, 450 °C, and 550 °C, respectively. Some OC is charred during the gradual increase in temperature and is defined as OP (pyrolyzed organic carbon). EC1, EC2, and EC3 are carbon fractions evolved under an O₂ atmosphere at 550 °C, 700 °C, and 800 °C, respectively, after OC/EC split.

^b In this study, the mean EC2+3 of PM_{1.0} (0.46) was a little higher than that of PM_{2.5} (0.40) and PM₁₀ (0.30). It is likely associated with the amount of catalytically active ions (Han et al., 2009a) and mineral oxides (Fung, 1990; Novakov and Corrigan, 1995; Elmquist et al., 2006). In particular, the presence of these components in coarse particles may lead to a catalytically mediated lowering of the activation energy for soot oxidation but not for char (Elmquist et al., 2006).

liberated in an oxygen-free environment until a temperature of >600 °C is attained, allowing it to be separated from the more volatile OC that evolves at lower temperatures. Eight fractions of carbon, including four fractions of OC (at 120 °C for OC1, at 250 °C for OC2, at 450 °C for OC3, and at 550 °C for OC4 in a He atmosphere), three fractions of EC (at 550 °C for EC1, at 700 °C for EC2, and at 800 °C for EC3 in a 2 % O₂/98 % He atmosphere), and OP, pyrolyzed (or charred) OC, were determined by this analysis method. OP is measured after the introduction of a He/O₂ atmosphere but before reflectance or transmittance returns to its initial value (Chow et al., 2005).

**Fig. 2.** Mean concentrations of mass, water-soluble ions, EC, and OC in PM_{1.0}, PM_{2.5}, and PM₁₀. Ions include SO₄²⁻, NO₃⁻, and Cl⁻ for anions and NH₄⁺, K⁺, Na⁺, Ca²⁺, and Mg²⁺ for cations.

In conjunction with chemical composition, BC concentration was determined by absorption at 7 wavelengths, 370, 450, 520, 590, 660, 880, and 950 nm, using an Aethalometer (AE-31, Magee Scientific Corp., USA) every 10 min. Scattering coefficients were obtained at 450 nm, 550 nm, and 700 nm by a Nephelometer (model 3563, TSI Inc., USA) every 10 min. For these measurements, ambient air was pulled through a sampling manifold without cut-points. These optical measurement data are available since January 2008. Gaseous pollutants, including O₃, NO₂, CO, and SO₂, and a meteorological suite were measured hourly by the National Institute of Environmental Research (NIER) and the Korea Meteorological Administration (KMA), respectively. These data were averaged hourly or daily for comparison with the chemical composition data.

3 Results and discussion

3.1 Size-fractionated ionic and carbonaceous compositions

The daily concentrations of PM_{1.0}, PM_{2.5}, and PM₁₀ varied between 1.3 and 29.5 μg m⁻³, 3.9 and 39.2 μg m⁻³, and 7.5 and 69.8 μg m⁻³, respectively. Mean mass concentrations

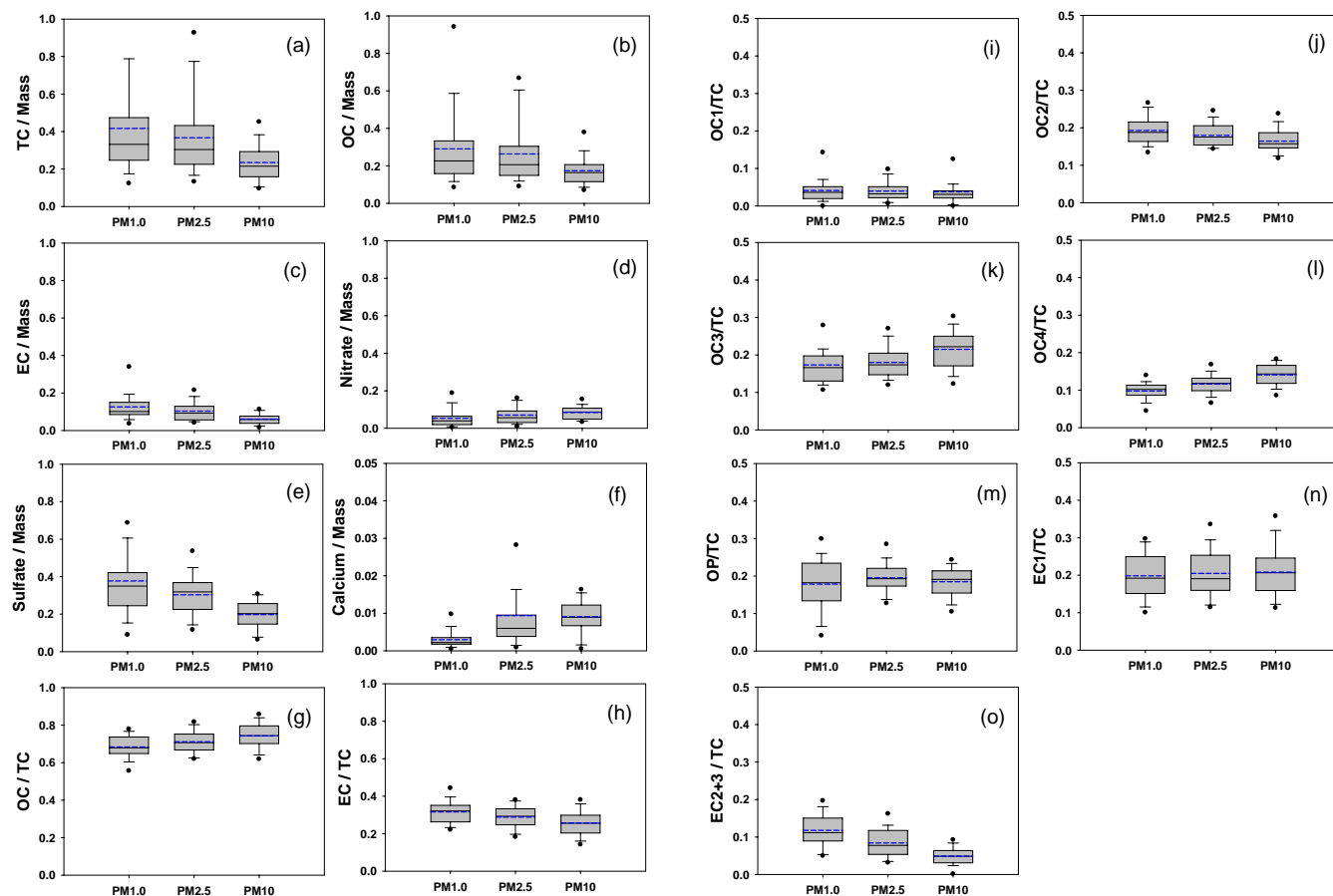


Fig. 3. Ratios of each chemical component to mass or total carbon (TC = OC + EC) in PM_{1.0}, PM_{2.5}, and PM₁₀: (a) total carbon-to-mass, (b) OC-to-mass, (c) EC-to-mass, (d) nitrate-to-mass, (e) sulfate-to-mass, (f) calcium-to-mass, (g) OC-to-TC, (h) EC-to-TC, (i) OC1-to-TC, (j) OC2-to-TC, (k) OC3-to-TC, (l) OC4-to-TC, (m) OP-to-TC, (n) EC1-to-TC, (o) EC2+3-to-TC. Total Carbon (TC) is the sum of OC and EC, which are the sum of 5 sub-components (OC1, OC2, OC3, OC4, and OP) for OC and 3 components (EC1, EC2, and EC3) for EC (Han et al., 2007, 2010). OP stands for pyrolyzed organic carbon. Solid and blue dotted lines within the box denote the median and the mean value, respectively, and the box represents the 25th and 75th percentiles. Whiskers above and below the box indicate the 90th and 10th percentiles, and solid circles are outliers corresponding to 5th and 95th percentiles of the data.

were $13.7 \mu\text{g m}^{-3}$ for PM_{1.0}, $17.2 \mu\text{g m}^{-3}$ for PM_{2.5}, and $28.4 \mu\text{g m}^{-3}$ for PM₁₀ (Fig. 2 and Table 2), suggesting that the daily mass well represented episodic events associated with pollution and dust plumes. Caution needs to be exerted when comparing these values with annual mean because there is relatively less number of samples during summer and winter monsoon periods. The noticeable feature was a large fraction of PM_{1.0} against PM₁₀ (48.4 %) and against PM_{2.5} (60.8 %) on average. PM_{2.5} accounted for 79.6 % of PM₁₀.

In particulate matter of all sizes, the most abundant constituents were water-soluble ions, which were followed by OC and EC (Fig. 2). We did not convert OC to OM, and the following discussion is pertinent only to OC. The concentrations of ions were almost twice as high as those of OC, and OC was nearly two times higher than EC. The average mass fractions of ions, OC, and EC were 53.9 %, 23.0 %, and 10.4 % for PM_{1.0}, 52.4 %, 22.9 %, and 9.8 % for PM_{2.5}, and 43.4 %, 16.4 %, and 6.0 % for PM₁₀, revealing that carbonaceous compounds were the most abundant in PM_{1.0} and PM_{2.5}. A considerable fraction of mass other than water-soluble ions, OC, and EC was possibly due to major, minor, and trace metals, including silica, which were not measured (Moon et al., 2008).

The ratios of OC/EC were 2.2, 2.3, and 2.8 for PM_{1.0}, PM_{2.5}, and PM₁₀, respectively. These mean OC/EC ratios were much lower than those measured at the regional background (RB) site in Western Mediterranean (~ 11 for PM_{2.5}) (Pey et al., 2009) and at two RB sites in western China (~ 12 for PM₁₀) (Qu et al., 2009), and still lower than those of many RB sites in Europe (OC/EC $> 2-3$) (Pey et al., 2009). Our OC/EC ratios were, however, comparable to those observed in Beijing and Shanghai regions (He et al., 2001; Ye et al., 2003). Although there are not significant local

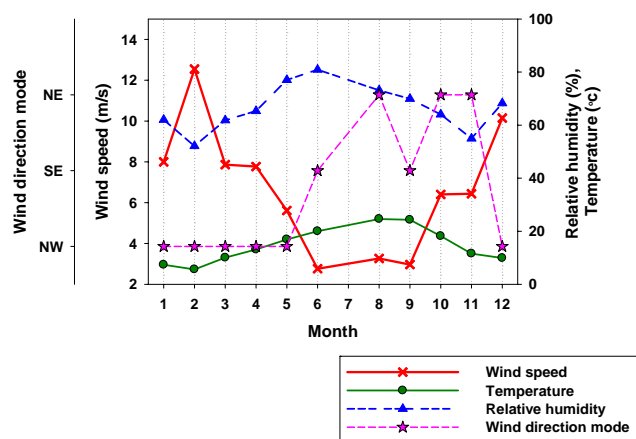


Fig. 4. Monthly variations of meteorological parameters including temperature, relative humidity, wind speed, and wind direction. Wind direction is represented as a mode divided into 8 from N to NW for 1-h data, and the wind mode in this study includes NE, SE, and NW.

emissions near Gosan station, its EC level is relatively higher than those of above RB sites because it is under direct influence of the northeast Asian outflows. Beijing and Shanghai are the main source regions of anthropogenic emissions affecting Gosan aerosols, which will be further discussed in Sect. 3.4. Therefore, the low OC/EC ratio in this study area likely indicates the effect of long range transport of urban plumes from China.

The distributions of TC/mass, OC/mass, and EC/mass among particle sizes were very similar, increasing with decrease in particle diameter (Fig. 3a, b, and c). The trends imply substantial anthropogenic influence and atmospheric processing such as condensation, gas-to-particle conversion, or surface-limited oxidation processes. With the low OC/EC ratio most of OC is anthropogenic. Additionally, EC/mass distributions were slightly sharper than OC/mass with decrease in particle size, indicating a larger contribution of EC to fine particles. For water-soluble ions, sulfate was the most abundant single species, and its concentration was comparable to that of TC, accounting for 20–30% of the mass (Fig. 3e). Also, the sulfate-to-mass ratio was found to be slightly more shifted toward PM_{1.0} than was the TC-to-mass ratio, while being similar in size distribution. This shift is probably due to a large amount of non-sea-salt sulfate (nss-SO₄²⁻) originating from anthropogenic sources, which contributed about ~75–99% of total sulfate aerosols, and is dependent on gas-to-particle conversion processes. The concentrations of none-sea-salt components were calculated from the measured sodium concentrations and the ratio of the component to sodium in seawater.

In contrast to the carbonaceous aerosols and the sulfate, significant differences in size distributions were observed for calcium and nitrate (Fig. 3d and f). These species were much

higher in PM₁₀ than in the other size fractions. In the case of nitrate, the next most abundant species among the water-soluble ions, this is due to its chemical and physical characteristics, especially its volatility. Ammonium nitrate, being more volatile than ammonium sulfate, will tend to evaporate from smaller particles and yield gaseous nitric acid which reacts onto coarser particles. Ammonium sulfate, being essentially non-volatile, has a size distribution controlled by gas-phase diffusion and will tend to accumulate in small particles (Bassett and Seinfeld, 1984). For calcium, its main sources are soils and sea salt in general; however, the soil-derived calcium would be a more abundant component of total calcium in the present study because non-sea-salt-calcium (nss-Ca²⁺) accounts for ~43–97% of the total calcium in all particle sizes. In previous studies, it has been suggested that nitrate is formed through heterogeneous reactions including nitrogen oxides and by absorption of nitric acid on the surface of soil particles (Mamane and Gottlieb, 1989; Zhang et al., 1994). At the Gosan station, the correlation between nitrate and calcium in PM₁₀ was significant ($R^2 = 0.51$) for all measurements, including the high PM₁₀ episodes that were affected by Asian dust event. The correlation implies that there is a mineral affinity of nitrate in coarse mode particles and that some of the nitrate could have been formed on dust particles enriched with calcium. In fact, there have been intensive studies on the link between anthropogenic nitrate or sulfate and mineral constituents of Asian dust (Wang et al., 2007; Lin et al., 2007; Geng et al., 2009) and Saharan dust particles (Talbot et al., 1986; Mace et al., 2003; Koçak et al., 2007). Particularly, Geng et al. (2009) reported that the nitrate-containing secondary soil-derived particles were markedly increased in coarse mode during Asian dust period. Asian dust was also suggested to provide a removal mechanism for NO_x (or HNO₃) and perhaps contribute to nitrogen deposition in the Yellow Sea (Wu and Okada, 1994).

The ratios of OC and EC to TC as a function of particle diameter (Fig. 3g and h) reflect the oxidation and condensation mechanisms of carbonaceous compounds. Gas-to-particle conversion and heterogeneous chemistry in the atmosphere control chemical and physical properties of aerosols, but these processes are not understood well enough to predict accurately the evolution of the gas and particle-phase composition of the troposphere (Ravishankara, 1997; Maria et al., 2004). In particular, the formation and the mixing state of carbonaceous aerosols are important due to their considerable anthropogenic source and high concentration. As shown in Fig. 3g and h, the EC-to-TC ratio increased with decrease in particle size, while the OC-to-TC ratio showed an opposite trend. Particles generated through condensation of hot vapor or from direct emissions can become oxidized through heterogeneous reactions that are surface-limited or volume-limited (Worsnop et al., 2002). EC particles were likely controlled by surface-limited processes in the study region because the localization of the reactions at the particle surfaces results in larger concentrations of carbon in smaller

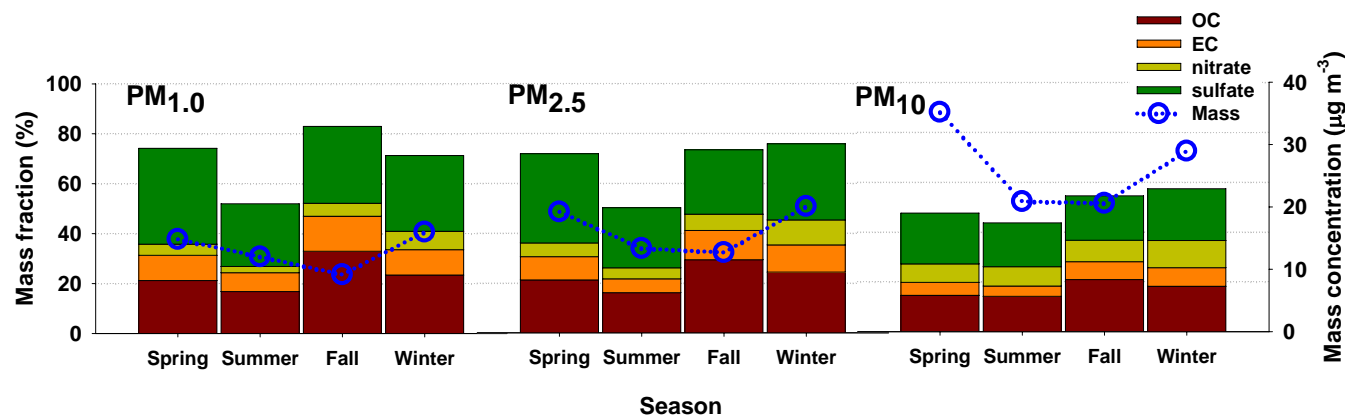


Fig. 5. Seasonal variations of mass concentrations (blue circle) and fractions of OC, EC, nitrate, and sulfate against mass in PM_{1.0}, PM_{2.5}, and PM₁₀. Spring, summer, fall, and winter include March to May, June to early September, October to November, and December to February, respectively.

aerosol particles with larger surface-to-volume ratios than larger particles (Maria et al., 2004). Although EC is mixed with organic compounds in the atmosphere, surface-limited oxidation may easily occur because organic compounds often have efficient surface reactivity (Maria et al., 2004; Russell et al., 2002). In the case of OC, interestingly, the OC/TC ratio was highest in the coarse mode and lowest in PM_{1.0}. The OC enrichment in coarse mode could be attributed to the formation of secondary organic aerosols (SOA) and subsequent increase in size during aging processes (Liu et al., 2009). The relatively higher OC/EC ratio (2.5 for PM_{2.5} and 3.3 for PM₁₀) in spring and summer implies SOA formation at higher temperature, even though OC concentrations were lower than those in winter. Mochida et al. (2007) performed size-segregated aerosol measurements off the coast of East Asia and found a high OC proportion in the supermicron mode of up to 61 %, suggesting primary emission of organics associated with sea salt and dust particles or other primary sources (e.g. plant waxes, soil-derived microbes, and anthropogenic particles). In this measurement, a similar behavior of OC and EC was observed during an Asian dust event in May 2008 (Lim et al., 2010a, b), in which the ratio of OC to EC was raised in dust-laden air possibly due to the impact of dust-related primary OC. Therefore, it is suggested that there was a considerable contribution of primary OC as well as SOA to total OC concentration particularly in the present study.

The ratios of OC and EC subcomponents to TC (Fig. 3i–o) were divided into three types. The first group includes OC1, OP, and EC1, whose ratios against TC did not show a clear tendency to vary with particle size (Fig. 3i, m, and n). OC1 may represent semi-volatile organic carbon because OC1 not only is the first carbon evolved at the lowest temperature but also is observed to be the most abundant and variable in concentration among the 5 OC fractions in our blank filters. OP is a measure of pyrolyzed organic carbon, and its character-

istics are well described by Andreae and Gelencsér (2006), who explained that OP can be released as a gas or in solid form and become associated with submicron or supermicron particles. Similarly, EC1 was defined as char EC (Han et al., 2010), and a detailed discussion of EC1 is given in Sect. 3.3. The second group includes OC2 and EC2+3, whose ratios to TC were enhanced in the smaller size particles (Fig. 3j and o). This enhancement strongly supports the view that a condensation process or surface-limited oxidation was involved in the formation of OC2 and EC2+3. Particularly, OC2 is thought to be a secondary organic carbon, which will be further discussed in Sect. 3.4. In contrast to OC2, the fractions OC3 and OC4 clearly increased with increasing particle size (Fig. 3k and l), and their concentrations were also higher in PM₁₀ than in PM_{1.0}, suggesting the characteristic of primary aerosols.

3.2 Seasonal patterns

The monthly variations of meteorological parameters include those of temperature, which varied between 4.4 °C and 25.8 °C, and relative humidity, which ranged from 37.2 % to 87.6 % over the whole period, showing distinct seasonal patterns. The mode of wind direction in degrees from 0° to 360° was chosen for each month and categorized into eight groups from N to NW. Throughout the winter and the spring, the prevailing wind was northwesterly under the influence of the winter monsoon over East Asia, with high wind speeds up to 13 m s⁻¹, suggesting a greater influence during that period from Asian continental outflows. With the arrival of summer, the wind direction was shifted to easterly with lower wind speeds below 3 m s⁻¹, indicating reduced continental outflows (Kim et al., 2007).

Seasonal mass fractions of major components (OC, EC, nitrate, and sulfate) and mass concentrations are compared in Fig. 5. The average PM_{1.0} and PM_{2.5} levels were highest

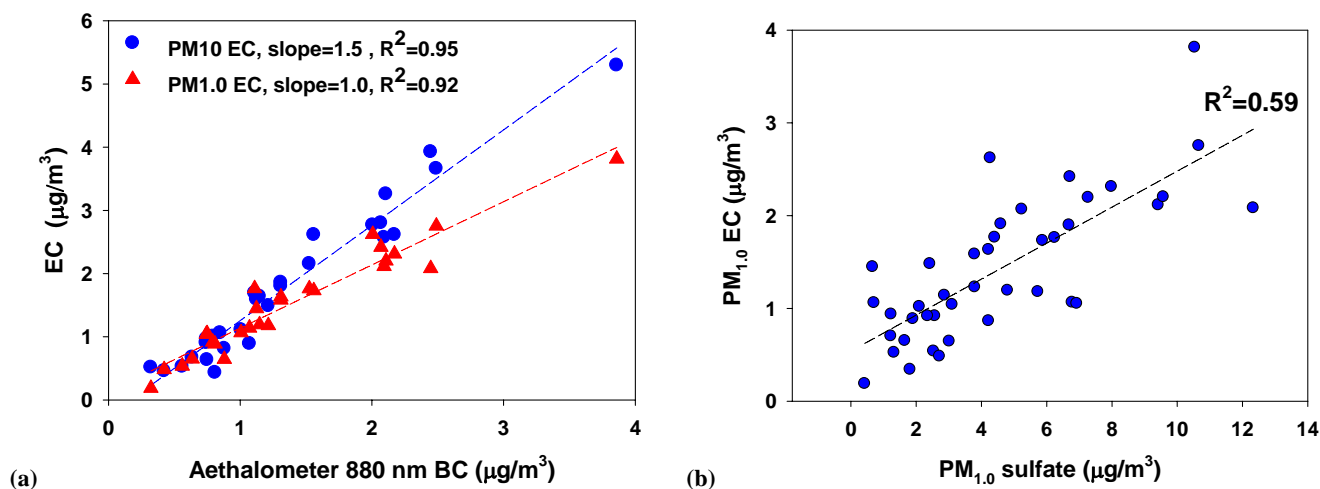


Fig. 6. Correlations of (a) BC measured by Aethalometer at 880 nm with EC in PM_{1.0} and PM₁₀ and (b) sulfate with EC in PM_{1.0}. The Aethalometer acquires data at seven wavelengths from the ultraviolet to near-infrared: 370, 470, 520, 590, 660, 880, and 950 nm. BC concentrations were averaged for 24 h in accordance with collection duration for filter samples. The dotted lines represent linear regression fits, for which R^2 values are given.

Table 3. Correlation coefficients of absorption and scattering properties of aerosols with EC and sulfate concentrations in PM_{1.0}.

	PM _{1.0} EC	PM _{1.0} sulfate
Aethalometer BC (520 nm) ^a	0.94	0.64
Scattering coefficient (550 nm) ^b	0.73	0.79

^a Aethalometer acquires data at seven wavelengths: 370, 470, 520, 590, 660, 880, and 950 nm.

^b Nephelometer acquires data at three wavelength: 450, 550, and 700 nm.

during winter at $16.3 \mu\text{g m}^{-3}$ and $20.3 \mu\text{g m}^{-3}$, respectively, followed by spring, when the highest seasonal PM₁₀ was observed ($35.2 \mu\text{g m}^{-3}$). The enhanced mass concentrations were associated with anthropogenic sources, mostly from the Asian continent during the winter monsoon season and with Asian dust events in the spring. The lowest mass concentrations at all sizes were due to frequent rain and small continental effects during the summer season (Lim et al., 2010a, b). While sulfate was most abundant during spring with a fraction of 20–38 %, nitrate was the highest during winter, with a fraction of 7–11 %. The occurrence of the highest sulfate fraction in spring compared with other seasons was due to the combination of enough SO₂ sources mainly from Asian continent and favorable ambient conditions for converting SO₂ to sulfate. In summer, on the other hand, sulfate concentrations were low because of the lowest SO₂ concentrations below 1.0 ppbv even under favorable conditions for sulfate conversion and wet removal of precursor gases and particles. Seasonal nitrate levels were inversely related to ambient temperature, being highest in winter at 7–11 %, moderate in spring and fall at 5–9 %, and lowest in summer at 3–8 %.

In this study, carbonaceous fractions were higher in summer and fall under low mass and sulfate concentrations but lower in winter and spring under high mass and sulfate concentrations. Particularly, the OC and EC fractions of PM_{1.0} were highest in fall. It is likely due to biomass burning from local farmlands and nearby continents as well. In spring, biomass burning also takes place but its effect is diluted by high anthropogenic emissions of sulfur and nitrogen.

3.3 Characteristics

The EC was compared with BC measured by Aethalometer (Fig. 6a). In contrast to EC quantification by thermochemical analysis, BC concentration was obtained by optical analysis, which estimates light absorption of particles and converts it into mass concentration using a mass specific attenuation cross-section of $16.6 \text{ m}^2 \text{ g}^{-1}$ at 880 nm (Magee BC calibration, Hansen, 2005). The slope of the regression equation of PM_{1.0} EC against BC at 880 nm was 1.0, whereas the slope for PM₁₀ EC against BC was 1.5. This result implies that mass absorption efficiency is higher for smaller particles and that the greater fraction of coarse EC may not absorb as much BC as fine EC does.

It can be seen in Fig. 6b that EC and sulfate were well correlated. Due to condensation processes or cloud processing, atmospheric EC is mixed with scattering aerosols (such as sulfate and organic carbon) and can acquire non-absorbing coatings. Although we cannot estimate its mixing state from our data, EC can be sufficiently mixed with sulfate in places under the influence of substantial anthropogenic sources. That is why sulfate shows not only a good correlation with scattering efficiency measured by Nephelometer but also a reasonable correlation with BC measured by

Aethalometer (Table 3). EC was also well correlated with scattering efficiency and BC. It has been shown that more hygroscopic particles, such as sulfate of a given size, will grow more under humid conditions, scattering more incident light (Jimenez et al., 2009). Other studies have reported Mie calculations of soot particles with sulfate coatings showing enhanced absorption (Martins et al., 1998; Fuller et al., 1999). These results suggest a positive contribution of sulfate coatings to net warming.

EC is not a single chemical compound. It can be subdivided into two classes based on our analytical method: char-EC and soot-EC (Han et al., 2007, 2010). Char was defined as carbonaceous material obtained by heating organics and formed directly from pyrolysis or as an impure form of graphitic carbon obtained as a residue when carbonaceous material is partially burned or heated with a limited supply of air. Soot was defined as only those carbon particles that form at high temperature via gas-phase processes. Previous studies showed that char and soot had different chemical and physical properties (Kuhlbusch, 1997; Masiello, 2004), as well as optical properties (Bond, 2001; Bond et al., 2002; Kirchstetter et al., 2004). We adopted the operational definitions of EC fractions that Han et al. (2010) suggested to demonstrate the different characteristics of char and soot, based on their previous lab experiment (Han et al., 2007). Their experiment result supported the use of the TOR method to discriminate between char- and soot-EC. The activation energy was lower for char- than soot-EC; char materials always oxidized at low-temperature (550 °C, at EC1 stage), while Diesel and n-hexane soot samples exhibited similar EC2 peaks (at 700 °C) and carbon black samples peaked at both EC2 and EC3 (800 °C). In our study, therefore, char-EC and soot-EC are operationally defined as EC1 and as EC2+3, respectively. In the present work, the mean EC1 concentrations were almost two times higher than the mean EC2+3 concentrations for all size cuts, ranging from 0.96 µg m⁻³ to 1.39 µg m⁻³ for EC1 and from 0.30 µg m⁻³ to 0.46 µg m⁻³ for EC2+3.

We compared the relationships between EC1 and EC2+3 in the different seasons. They showed the strongest correlation in winter and spring ($R^2 = 0.4\text{--}0.6$ for PM_{1.0}, PM_{2.5}, and PM₁₀), which suggests common combustion sources such as biomass burning, residential heating, and coal combustion. In contrast, they were poorly correlated in summer ($R^2 = 0.03\text{--}0.2$ for PM_{1.0}, PM_{2.5}, and PM₁₀), which was likely due to reduced sources, particularly from biomass burning and residential heating. Furthermore, the overall correlation between EC1 and EC2+3 was better in PM₁₀ rather than PM_{1.0}. This seems to be associated with particle size: EC1 has larger size (~1–100 µm) than EC2+3, which is emitted as gas or smaller particles (~hundreds of nm).

Although, generally, the concentration of aerosols in the study area is mainly determined by emissions from the Asian continent, transport processes and wet scavenging have an effect on the level of each aerosol component. Here, we ex-

Table 4. The ratios of EC1 and EC23 concentrations for non-rainy days to those for rainy days in PM_{1.0}, PM_{2.5}, and PM₁₀.

Non-rainy days ($N = 31$)/ Rainy days ($N = 10$)	PM _{1.0}	PM _{2.5}	PM ₁₀
EC1	1.5	1.8	1.5
EC2+3	1.0	1.1	1.3

amined the impact of precipitation on the mass difference between EC1 and EC2+3 using the ratio of the concentration during non-rainy days (31 days) to the concentration during rainy days (10 days) (Table 4). EC2+3 showed little wet scavenging effect with a ratio of 1.0 ~ 1.3. On the other hand, EC1 had a difference in concentration between non-rainy and rainy days. These results imply a longer residence time of EC2+3 in the atmosphere, meaning that soot aerosols are suspended and transported longer. In general, since char-EC is composed of large particles (>~1 µm) as well as small particles, it could be easily removed by wet deposition. Soot, consisting of submicron particles of grape-like clusters, may have an atmospheric lifetime of a month (Ogren and Charlson, 1983) and has strong light absorption characteristics with little spectral dependence (Schnaiter et al., 2003; Kirchstetter et al., 2004). Thus soot could have greater consequence for warming.

The soot-EC/char-EC ratio depends upon the mixing function of the different sources: motor vehicle emissions and possibly grass burning result in higher soot-EC/char-EC ratios, while wood combustion, particularly biomass burning by smoldering at low temperature, produces lower soot-EC/char-EC ratios (Chow et al., 2004; Chen et al., 2007). In coal combustion, this ratio can be very low or relatively high, depending on the type of coal (Han et al., 2010). To apply the definitions of Han et al. (2010) to our study, we compared seasonal EC2+3/EC1 ratios (Fig. 7). Seasonally averaged EC1 concentration was highest in winter and lowest in summer. This order is very well matched with the intensity of continental outflows. In contrast, EC2+3 did not show clear seasonal variation, but the highest concentrations were found in spring and the lowest concentrations in fall and winter. As a result, the ratios of EC2+3/EC1 were highest in summer, when air masses reached at Gosan from the east passing through South Korea or/and Japan with the least influence by the continent and greater influence by South Korea and Japan (see Fig. 9e). In fact, the EC2+3/EC1 ratio of 1.25 in summer is comparable to the ratio of 1.67 for motor vehicle exhaust (Chow et al., 2004). EC2+3 emitted during winter and spring may have remained suspended in the atmosphere due to its smaller size and kept its proportion through increased motor vehicle sources from South Korea and Japan, in spite of the wet scavenging caused by frequent precipitation during summer. Han et al. (2010) collected PM_{2.5} EC particles in Xi'an,

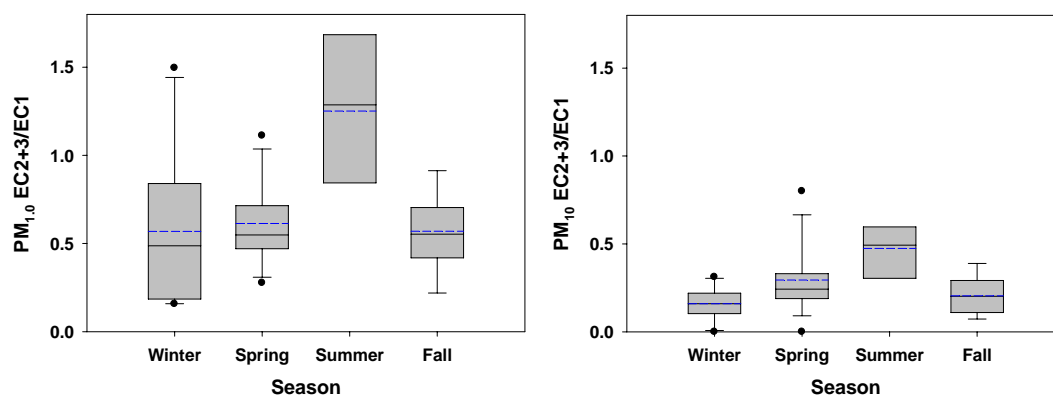


Fig. 7. Seasonal variations of soot-EC to char-EC in PM_{1.0} and PM₁₀. See Fig. 3 for the detailed explanation of box and whisker plot.

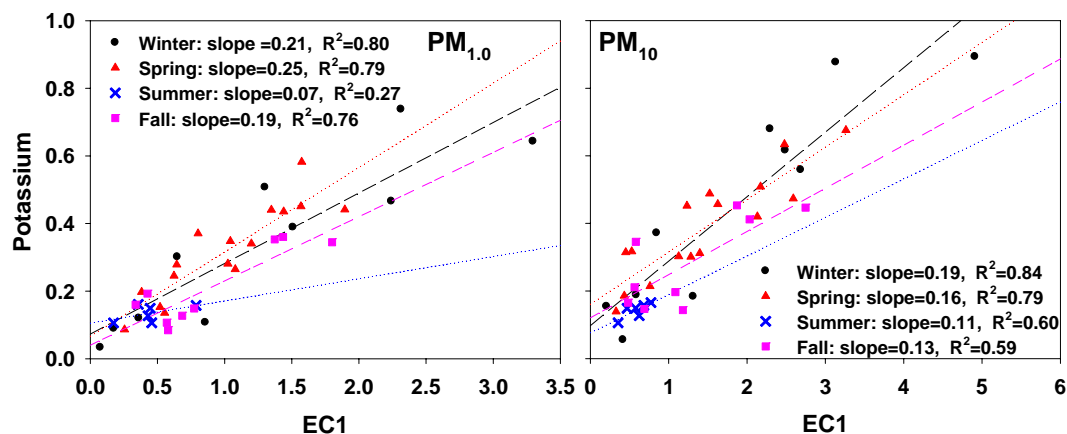


Fig. 8. Correlations of EC1 with potassium for PM_{1.0} and PM₁₀ in each season. Lines stand for linear regression fittings, for which slopes and R^2 values are given.

a sandland in China, of which result were consistent with our observation that EC1 had a minimum level in summer, but in contrast to our observations, the level of EC2+3 was also minimum in summer. Higher EC2+3 concentrations during summer in our data imply increased influence of South Korea and Japan on EC concentrations. Hence, EC2+3 is considerably enhanced, but EC1 is markedly less because of limited contact with industrial regions in China. In other study by Han et al. (2009b) that measured PM_{2.5} EC in 14 Chinese cities during summer and winter period, the lower ratios of EC2+3/EC1 were found at the sites associated with industries in the Eastern coastal region of China, while the opposite trend was observed at the sites in Northern and Southern China with the least industrial effect. Therefore, our study supports the classification of char-EC and soot-EC proposed by Han et al. (2010), and the ratio of EC2+3 to EC1 can serve as an indication of a continental effect. This result agrees well with air mass trajectories, which will be discussed in the following section. For example, the EC2+3/EC1 ratios for the days shown in Fig. 9 are (a) 0.96, (b) 0.17, (c) 0.32, (d) 0.47, and (e) 1.79.

Except for summer, EC1 was closely correlated with potassium, which, among the water-soluble ions, is traditionally well known as an indication of biomass burning (Silva et al., 1999; Guazzotti et al., 2003). Because char-EC has a wide variety of sources and its concentration itself does not provide accurate information about the source, this approach can suggest the contribution of biomass burning to EC1 concentration in different seasons. For the whole measurements, non-sea-salt potassium (nss-K⁺) accounted for ~50–99 %, which could be associated with mineral dust as well as combustion aerosols. In PM₁₀, nss-K⁺ was well correlated with nss-SO₄²⁻ ($R^2 = 0.70$), but moderately correlated with nss-Ca²⁺ ($R^2 = 0.53$). In addition, nss-K⁺ and nss-SO₄²⁻ showed similarity in size distribution of being enriched in fine mode. Among OC sub-components, OC2, thought to be secondary, was significantly correlated with sulfate and potassium. In the airborne measurements of trace elements produced from savanna biomass burning, Gaudichet et al. (1995) indicated that near the emission, K was mainly present as KCl, evolving to K₂SO₄ in the ambient samples. Thus, our potassium would be likely to represent the effect

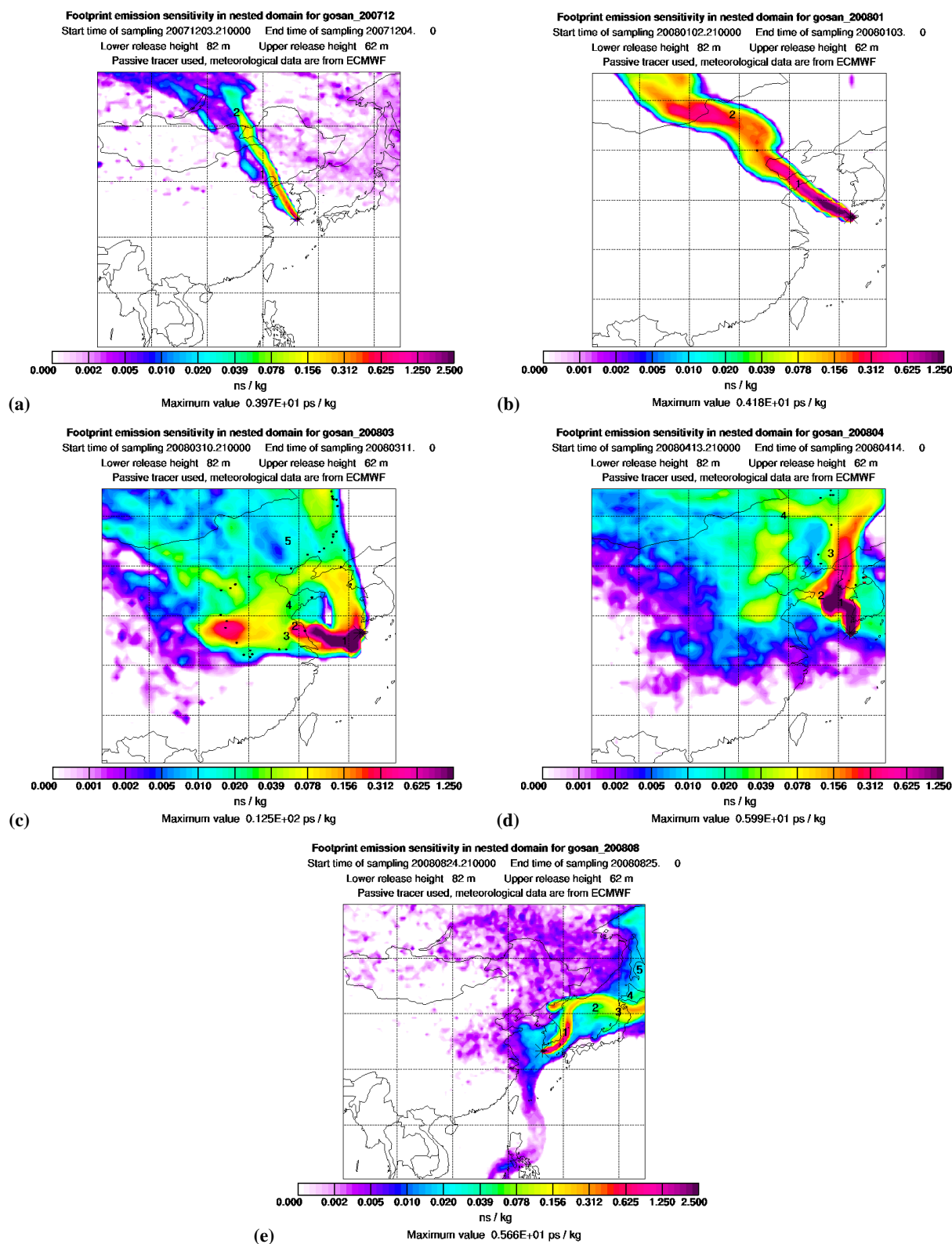


Fig. 9. Five air mass trajectories representing the influence from (a) Siberia region (e.g. 4 December 2007), (b) Beijing region (e.g. 3 January 2008), (c) Shanghai region (e.g. 11 March 2008), (d) Yellow Sea region (e.g. 14 April 2008), and (e) East Sea region (e.g. 25 August 2008). Backward trajectories were calculated every 3 h using the Lagrangian particle dispersion model FLEXPART (Stohl et al., 2005; <http://zardozi.nilu.no/~andreas/STATIONS/GOSAN/index.html>). The model output (s kg^{-1}) is a potential emission sensitivity distribution of 40 000 particles released in a particular grid cell at the measurement location and during the measurement interval and followed backward in time, which is proportional to the particle residence time in that cell.

of biomass burning, even if it may include some of fossil fuel combustion, dust, and sea salt as well.

Li et al. (2006) quantified EC and OC concentrations in Horquin sandland in northeastern China by a thermal method and reported the strongest correlation of EC with potassium among five elements, suggesting a significant contribution of rural biomass burning to regional carbonaceous aerosol concentrations. A previous study estimated the emissions of BC in China and pointed out that biomass burning is one of the main sources of BC in China (Streets et al., 2003). Gustafsson et al. (2009) used ¹⁴C to distinguish fossil fuel and biomass-burning contributions to BC during pollution events in South Asia. They found a far larger contribution of biomass combustion to BC emissions. Biomass burning is dominated on a global scale by fires due to slash-and-burn land clearance, waste burning in agriculture and forestry, and residential wood combustion for heating and cooking (Sizdat et al., 2009). In particular, East Asia contains biomass burning sources in undeveloped regions of China, Siberia, and North Korea. Biomass combustion-derived materials are likely generated throughout, with the strongest correlations in winter and spring, and transported to the study area. In summer, it is possible that reduced burning and relatively increased sea-salt potassium (ss-K⁺) lead to a poor correlation between EC1 and potassium, and that EC1 may deposit on the surface of larger and hygroscopic ss-K⁺, leading to better correlation in PM₁₀ than PM_{1.0}. It is less likely that Siberian wildfires or biomass burning in eastern China had influence on EC1 level of summer samples (Kim et al., 2007).

3.4 Source areas

To examine the source signature of aerosols and the effect of transport paths on aerosol composition, we categorized air masses into 5 regimes based on meteorological and chemical characteristics and air mass trajectories every 3 h using the FLEX-PART Lagrangian particle dispersion model (Stohl et al., 2005) (Fig. 9). In this analysis, samples which were affected by precipitation or did not show constant trajectories in time were excluded. The five types are labeled “Siberia”, “Beijing”, “Shanghai”, “Yellow Sea”, and “East Sea” according to the major geographical regions over which an air mass passed during transport. The Siberia, Beijing, Shanghai, Yellow Sea, and East Sea types included 6 days from October to March, 10 days from October to May, 4 days from October to May, 2 days in April, and 6 days from June to September, respectively. The characteristic regimes of each air type are summarized in Table 5. It should be noted that the study region is heavily affected by the monsoon system, and stagnant conditions often developed during transition periods, when trajectories tended to spread over wider areas.

From late fall to early spring, the study region is under the influence of frontal system in association with a Siberian high that is periodically extends towards the southeastern China. As a high pressure approaches, air is usually trans-

ported directly from Siberia to Jeju along with a trough. Then high pressure center shifts its way to the southeast and wind turns to northwesterly. While the former represents the continental background air descending from the free troposphere in Siberian region, the latter is classified as Beijing type air that passed fast over Mongolia and Beijing region. As the high pressure is weakened, the air slowly moves down to the southern part of China or over the Yellow Sea before reaching Gosan. The former is classified as Shanghai type that captured the emissions from the southern (Shanghai) as well as northern (Beijing) part of China. The latter is Yellow Sea that is mainly influenced by the Bohai Bay area and in part the west coast of the Korean peninsula. The air mass labeled East Sea was influenced by the East Sea, including Japan and South Korea, and was the most frequently observed air mass in summer. Siberia type can be regarded as clean background air of the northeast Asia (Fig. 9a). The Beijing and Shanghai types represent fresh continental and aged continental plume, respectively (Fig. 9b and c). As being aged over the ocean, the Yellow Sea type exhibits characteristics of continental plumes (Fig. 9d) and is distinguished from East Sea type air (Fig. 9e).

For each air mass category, the ratios of major constituents in submicron and supermicron aerosols are compared in Table 6. Siberia air showed the lowest levels of CO, sulfate, and PM_{1.0} mass concentrations, resulting in high ratios of chemical constituents. In Beijing type air, the ratios of OP, EC1, and nitrate to mass were the highest. In contrast, an enhanced sulfate/mass ratio was recognizable in Shanghai and Yellow Sea air masses. For these two air masses, the high sulfate content was the result of favorable meteorological conditions such as weak winds and high relative humidity over a warm sea surface (Fig. 9c and d) (Lim et al., 2010a, b) in conjunction with sources from nearby land. The higher nitrate/sulfate ratios in Beijing type air mass are largely due to the temperature dependency of nitrate because the Beijing air was more frequently encountered at Gosan in the colder seasons. Therefore, Beijing and Shanghai plumes were unambiguously differentiated by the ratios of EC1, OP, and nitrate against sulfate.

It is noteworthy that the OC2 fraction against total carbon was also much higher in the Yellow Sea and East Sea types, which could be characterized as relatively aged marine air masses (Fig. 9d and e). It is supporting evidence for the secondary nature of OC2, such that its ratio to TC tended to be higher in the smaller particle sizes (Fig. 3j). In addition, the ratio of EC2+3 to EC1 was distinctly higher in the East Sea air mass. This result agrees with the findings of Han et al. (2010) and this study that the ratio of EC2+3 to EC1 can serve as an indicator of continental effects and suggests a greater influence of motor vehicle emissions from South Korea and Japan, with a reduced influence from China. This ratio is also likely to be increased in aged air due to the longer lifetime of EC2+3 than EC1, as discussed in the previous section.

Table 5. Meteorological and chemical characteristics of the 5 air mass categories.

	Siberia	Beijing	Shanghai	Yellow Sea	East Sea
Meteorology					
Wind speed (m s ⁻¹)	8.7	7.3	4.6	3.9	3.1
Temperature (°C)	11.6	11.8	14.1	14.3	23.8
Relative humidity (%)	56.6	57.5	57.5	76.2	73.4
Gases (ppbv)					
CO	501	648	533	527	613
SO ₂	1.7	5.3	5	2	0.5
NO ₂	NA ^a	4.9 ^b	NA ^a	4.2	4.1
O ₃	44.3	46.8	65.1	64.2	41.0
Particles (µg m ⁻³)					
PM _{1.0}					
Mass	7.5	15.2	24.1	22.8	12.3
Nitrate	0.4	0.9	1.8	1.0	0.3
Sulfate	2.0	4.9	10.0	8.7	3.1
TC	3.5	6.0	6.9	5.9	3.0
OC2	0.7	1.0	1.3	1.2	0.7
OP	0.7	1.5	1.4	1.0	0.3
EC1	0.6	1.4	1.8	1.5	0.4
EC2+3	0.4	0.4	0.5	0.8	0.5
PM ₁₀					
Mass	23.2	35.9	42.8	40.8	20.9
Nitrate	1.7	3.4	4.3	2.9	1.6
Sulfate	2.8	5.9	11.2	10.7	3.7
TC	4.9	8.4	10.7	7.6	3.8
OC2	0.8	1.2	1.6	1.4	0.8
OP	0.9	1.8	2.1	1.4	0.7
EC1	0.8	1.9	2.9	2.2	0.6
EC2+3	0.2	0.3	0.5	0.4	0.3

^a NA: not available. ^b NA on 14 February and 3 April.

In the present study, OP was recognized as a major component of OC and found to be a source signature of the Beijing type air mass. Through the entire period of observation, OP was noticeably elevated when wind speed was high under the influence of a strong continental high or a migratory cyclone. As a result, high ratios of OP to EC1 were observed in fast-moving air parcels carried by northwesterly winds in winter or northerly winds in spring, which could bring relatively fresh emissions from Beijing and its vicinity and plumes due to biomass burning in Mongolia (Kim et al., 2007) and Siberia if they existed (Fig. 9a). In contrast, OP remained low in the warmer seasons, which were characterized by stagnant air masses, leading to low OP/EC ratios. These variations are evident in Table 6, in which it can be seen that the ratio of OP/EC1 was quite low in Yellow Sea and East Sea air masses. Therefore, the main sources of OP are likely to be coal combustion and biomass burning.

OP is defined as charred OC having characteristics similar to those of EC1 that absorbs light. The BC absorption spectrum measured by Aethalometer revealed different tendencies among 7 wavelengths, for some of which the absorption of short wavelength (370 nm) was greater than that of longer wavelengths. It is generally known that soot, which is composed of submicron particles of grape-like clusters, exhibits strong light absorption characteristics with little spectral dependence (Schnaiter et al., 2003; Kirchstetter et al., 2004). In the present study, the enhanced absorption of shortwave radiation was clear for samples containing large amounts of OP, implying the link between OP and light-absorbing organic carbon.

Table 6. Ratios of major chemical constituents indicating source regions categorized into 5 regimes: Siberia, Beijing, Shanghai, Yellow Sea, and East Sea.

Ratio	PM _{1.0}					PM ₁₀				
	Siberia	Beijing	Shanghai	Yellow Sea	East Sea	Siberia	Beijing	Shanghai	Yellow Sea	East Sea
OP/Mass	↑	↑	–	–	–	↑	↑	–	–	–
EC1/Mass	↑↑	↑	–	–	–	↑	↑	↑	–	–
Nitrate/Mass	↑	↑	↑	–	–	–	↑	↑	–	–
Sulfate/Mass	–	–	↑	↑	–	–	–	↑	↑	–
Nitrate/Sulfate	↑	–	–	–	–	↑	↑	–	–	–
OC2/TC	–	–	–	↑	↑	–	–	–	↑	↑
EC2+3/EC1	↑	–	↑	–	↑↑	–	–	↑	–	↑↑
OP/Sulfate	↑↑	↑	–	↓	↓	↑	↑	–	–	–
EC1/Sulfate	↑	↑	–	–	–	↑	↑	–	–	–

The ratios are expressed as symbols: ↑↑ for values larger than mean $\times 1.5$, ↑ for those between mean and mean $\times 1.5$, – for those between mean $\times 0.5$ and mean, and ↓ for those smaller than mean $\times 0.5$.

Although EC and BC have long been major topics of research due to their light-absorbing characteristics, the recent discovery of light-absorbing organic carbon makes it imperative to reassess and redefine the components that make up light-absorbing carbonaceous matter in the atmosphere (Andreae and Gelencsér, 2006; Alexander et al., 2008). There is a continuum of carbonaceous substances in atmospheric aerosols, where refractory organics included in a thermochemical classification are consistent with colored organics in an optical classification. These so-called brown carbons have a sharply increased absorption efficiency toward shorter wavelengths, although the absorption is much less than that of soot carbon at the wavelength of 550 nm, and this spectral dependence causes the material to appear brown and makes their absorption in the UV potentially significant due to the large amounts occurring in continental aerosols (Kirchstetter et al., 2004; Hoffer et al., 2006). However, their optical properties, origin, and chemical composition are poorly understood and thus need further investigation.

The results discussed above highlight the fact that the Beijing air mass is distinguished not only by higher ratios of EC1 and OP to mass but also by higher ratios of EC1 (and OP) to sulfate. This implies that air masses from the Beijing area may have a more significant influence on net warming than do air masses from the other regions. This result confirms the main conclusion of Ramana et al. (2010), who estimated the impact of BC/sulfate ratios of air masses transported from the Beijing and Shanghai areas on net warming based on surface and aircraft measurements conducted over the Yellow Sea in spring and summer.

4 Conclusions

Daily PM_{1.0}, PM_{2.5}, and PM₁₀ samples were taken at Gosan ABC Superstation on Jeju Island from August 2007 to September 2008. The mass concentrations of PM_{1.0}, PM_{2.5}, and PM₁₀ varied between 1.3 and 29.5 $\mu\text{g m}^{-3}$, 3.9 and 39.2 $\mu\text{g m}^{-3}$, and 7.5 and 69.8 $\mu\text{g m}^{-3}$, respectively. PM_{1.0} and PM_{2.5} account for 48.4 % and 79.6 % of PM₁₀, respectively, indicating a large portion of fine-mode aerosols in this study area. EC tended to be enriched in smaller particles and made up 10.4 %, 9.8 %, and 6.0 % of PM_{1.0}, PM_{2.5}, and PM₁₀, respectively. Unlike EC, OC accounted for 23.0 %, 22.9 %, and 16.4 % in PM_{1.0}, PM_{2.5}, and PM₁₀, respectively. The size distributions of OC subcomponents such as OC3 and OC4 reflected substantial contributions of primary sources such as dust, sea salt, or biogenic matter.

The definition and measurement techniques for atmospheric EC (or BC) have long been subjects of scientific controversy. We compared our observed EC with BC measurements obtained by Aethalometer and found a perfect relationship with a slope of 1.0 for PM_{1.0} EC1 (but not for PM₁₀). This result indicates that coarse particles have lower light-absorbing efficiency than fine particles. In our data, EC and sulfate were well correlated, meaning that there is difficulty in distinguishing absorbing aerosols from scattering aerosols. For EC, the definition of EC1 as char-EC and EC2+3 as soot-EC applied well to our measurements; the former is emitted from smoldering combustion (such as biomass burning and residential and coal combustion), and the latter is generated from flaming combustion (such as motor vehicle exhaust and coal combustion). The mean EC1 concentrations were almost two times higher than the mean EC2+3 concentrations for all three particle sizes, ranging from 1.0 $\mu\text{g m}^{-3}$ to 1.4 $\mu\text{g m}^{-3}$ for EC1 and from 0.3 $\mu\text{g m}^{-3}$ to 0.5 $\mu\text{g m}^{-3}$

for EC2+3. EC1 was strongly correlated with potassium throughout the year except for summer. While EC2+3 was more enriched in PM_{1.0}, EC1 favored PM_{2.5} or PM₁₀. As a result, EC1 was more sensitive to wet scavenging, and the ratio of EC1 to EC2+3 was higher in summer. This difference was likely linked with a longer residence time of EC2+3 than that of EC1 in the atmosphere. This result implies a role of EC2+3 as a contribution to warming, particularly at a regional scale, due to its longer lifetime, even though its concentrations in the atmosphere are lower.

This study highlights the ratios of major chemical species as useful tools to distinguish the main sources of aerosols and the degree of atmospheric processing. Five air mass types were clearly identified: Siberia, Beijing, Shanghai, Yellow Sea, and East Sea types. Siberian types would be regarded as continental background air of the northeast Asia. While the Beijing, Shanghai, and Yellow Sea air masses were mostly influenced by China, the Korean emissions affected the Yellow Sea and East Sea type air masses. For the East Sea air, Japanese and Korean influences were dominant. The Beijing type air was the freshest and was distinguished by higher concentrations of EC and OP relative to sulfate, signifying a higher net warming effect of aerosols in this air type than in the other three types. OP was also suggested as a light-absorbing form of carbon. On the other hand, sulfate was remarkably enhanced in air that had been slowly transported over China or the Yellow Sea, which was the case of the Shanghai and Yellow Sea air masses. The aged air masses of Yellow Sea and East Sea types in particular showed lower OP to sulfate ratios and higher OC2 to TC ratios. The latter implies a secondary role among OC fractions in conjunction with a tendency of enrichment at smaller aerosol sizes. Furthermore, the highest ratio of EC2+3 to EC1 was found in the East Sea air, in sharp contrast with the other air mass categories, which showed less impact of Chinese emissions.

Acknowledgements. Authors thank to A. Stohl for allowing us to use Flexpart results at Gosan. This study was supported by the Korea Research Foundation grant KRF-2008-314-C00402 and Research Agency for Climate Science grant RACS 2010-1007.

Edited by: X. Querol

References

Aggarwal, S. G. and Kawamura, K.: Carbonaceous and inorganic composition in long-range transported aerosols over northern Japan: Implication for aging of water-soluble organic fraction, *Atmos. Environ.*, 43, 2532–2540, 2009.

Akimoto, H.: Global Air Quality and Pollution, *Science*, 302, 1716–1719, doi:10.1126/science.1092666, 2003.

Alexander, D. T. L., Crozier, P. A., and Anderson, J. R.: Brown Carbon Spheres in East Asian Outflow and Their Optical Properties, *Science*, 321, 833–836, doi:10.1126/science.1155296, 2008.

Andreae, M. O. and Gelencsér, A.: Black carbon or brown carbon? The nature of light-absorbing carbonaceous aerosols, *At-*

mos. Chem. Phys., 6, 3131–3148, doi:10.5194/acp-6-3131-2006, 2006.

Andrews, E., Saxena, P., Musarra, S., Hildemann, L. M., Koutrakis, P., McMurry, P. H., Olmez, I., and White, W. H.: Concentration and composition of atmospheric aerosols from the 1995 SEAVS experiment and a review of the closure between chemical and gravimetric measurements, *J. Air Waste Manage. Assoc.*, 50, 648–664, 2000.

Bassett, M. E. and Seinfeld, J. H.: Atmospheric equilibrium model of sulfate and nitrate aerosols-II. Particle size analysis, *Atmos. Environ.*, 18, 1163–1170, 1984.

Bond, T. C.: Spectral dependence of visible light absorption by carbonaceous particles emitted from coal combustion, *Geophys. Res. Lett.*, 28, 4075–4078, doi:10.1029/2001GL013652, 2001.

Bond, T. C., Covert, D. S., Kramlich, J. C., Larson, T. V., and Charlson, R. J.: Primary particle emissions from residential coal burning: Optical properties and size distributions, *J. Geophys. Res.*, 107, 8347, doi:10.1029/2001JD000571, 2002.

Bond, T. C., Habib, G., and Bergstrom, R. W.: Limitations in the enhancement of visible light absorption due to mixing state, *J. Geophys. Res.*, 111, D20211, doi:10.1029/2006JD007315, 2006.

Bond, T. C., Bhardwaj, E., Dong, R., Jogani, R., Jung, S., Roden, C., Streets, D. G., and Trautmann, N. M.: Historical emissions of black and organic carbon aerosols from energy-related combustion, 1850–2000, *Global Biogeochem. Cy.*, 21, GB2018, doi:10.1029/2006GB002840, 2007.

Brasseur, G. P., Orlando, J. J., and Tyndall, G. S.: *Atmospheric Chemistry and Global Change*. Oxford University Press., Oxford, UK, 654, 1999.

Buzorius, G., McNaughton, C. S., Clarke, A. D., Covert, D. S., Blomquist, B., Nielsen, K., and Brechtel, F. J.: Secondary aerosol formation in continental outflow conditions during ACE-Asia, *J. Geophys. Res.*, 109, D24203, doi:10.1029/2004JD004749, 2004.

Cao, J. J., Wu, F., Chow, J. C., Lee, S. C., Li, Y., Chen, S. W., An, Z. S., Fung, K. K., Watson, J. G., Zhu, C. S., and Liu, S. X.: Characterization and source apportionment of atmospheric organic and elemental carbon during fall and winter of 2003 in Xi'an, China, *Atmos. Chem. Phys.*, 5, 3127–3137, doi:10.5194/acp-5-3127-2005, 2005.

Carmichael, G. R., Zhang, Y., Chen, L. L., Hong, M. S., and Ueda, H.: Seasonal variation of aerosol composition at Cheju Island, Korea, *Atmos. Environ.*, 30, 2407–2416, 1996.

Carmichael, G. R., Hong, M. S., Ueda, H., Chen, L. L., Murano, K., Park, J. K., Lee, H. G., Kim, Y., Kang, C., and Shim, S.: Aerosol composition at Cheju Island, Korea, *J. Geophys. Res.*, 102, 6047–6061, doi:10.1016/1352-2310(95)00230-8, 1997.

Chen, L.-L., Carmichael, G. R., Hong, M., Ueda, H., Shim, S., Song, C. H., Kim, Y. P., Arimoto, R., Prospero, J., Savoie, D., Murano, K., Park, J. K., Lee, H., and Kang, C.: Influence of continental outflow events on the aerosol composition at Cheju Island, South Korea, *J. Geophys. Res.*, 102, 28551–28574, doi:10.1029/97JD01431, 1997.

Chen, L.-W. A., Moosmuller, H., Arnott, W. P., Chow, J. C., Watson, J. G., Susott, R. A., Babbitt, R. E., Wold, C. E., Lincoln, E. N., and Hao, W. M.: Emissions from laboratory combustion of wildland fuels: Emission factors and source profiles. *Environ. Sci. Technol.*, 41, 4317–4325, 2007.

Chow, J. C., Watson, J. G., Kuhns, H. D., Etyemezian, V.,

- Lowenthal, D. H., Crow, D. J., Kohl, S. D., Engelbrecht, J. P., and Green, M. C.: Source profiles for industrial, mobile, and area sources in the Big Bend Regional Aerosol Visibility and Observational (BRAVO) Study, *Chemos.*, 54, 185–208, doi:10.1016/j.chemosphere.2003.07.004, 2004.
- Chow, J. C., Watson, J. G., Louie, P. K., Chen, L. W., and Sin, D.: Comparison of PM_{2.5} carbon measurement methods in Hong Kong, China, *Environ. Pollut.*, 137, 334–344, 2005.
- Decesari, S., Facchini, M. C., Matta, E., Mircea, M., Fuzzi, S., Chughtai, A. R., and Smith, D. M.: Water soluble organic compounds formed by oxidation of soot, *Atmos. Environ.*, 36, 1827–1832, 2002.
- Dentener, F. J., Carmichael, G. R., Zhang, Y., Lelieveld, J., and Crutzen, P. J.: Role of mineral aerosol as a reactive surface in the global troposphere. *J. Geophys. Res.*, 101, 22869–22889, doi:10.1029/96JD01818, 1996.
- Elmquist, M., Cornelissen, G., Kukulska, Z., and Gustafsson, Ö.: Distinct oxidative stabilities of char versus soot black carbon: Implications for quantification and environmental recalcitrance, *Global Biogeochem. Cycles*, 20, GB2009, doi:10.1029/2005GB002629, 2006.
- Fuller, K. A., Malm, W. C., and Kreidenweis, S. M.: Effects of mixing on extinction by carbonaceous particles, *J. Geophys. Res.*, 104, 15941–15954, 1999.
- Fung, K. K.: Particulate carbon speciation by MnO₂ oxidation. *Aerosol Sci. Technol.*, 12, 122–127, 1990.
- Gaudichet, A., Echalar, F., Chatenet, B., Quisefit, J. P., Malingre, G., Cachier, H., Artaxo, P., Maenhaut, W., and Buat-Ménard, P.: Trace elements in tropical African savannah biomass burning aerosol, *J. Atmos. Chem.*, 22, 19–39, 1995.
- Geng, H., Park, Y., Hwang, H., Kang, S., and Ro, C.-U.: Elevated nitrogen-containing particles observed in Asian dust aerosol samples collected at the marine boundary layer of the Bohai Sea and the Yellow Sea, *Atmos. Chem. Phys.*, 9, 6933–6947, doi:10.5194/acp-9-6933-2009, 2009.
- Gray, H. A., Cass, G. R., Huntzicker, J. J., Heyerdahl, E. K., and Rau, J. A.: Characteristics of atmospheric organic and elemental carbon particle concentrations in Los Angeles, *Environ. Sci. Technol.*, 20, 580–582, doi:10.1021/es00148a006, 1986.
- Guazzotti, S. A., Suess, D. T., Coffee, K. R., Quinn, P. K., Bates, T. S., Wisthaler, A., Hansel, A., Ball, W. P., Dickerson, R. R., Neusüß, C., Crutzen, P. J., Prather, K. A.: Characterization of carbonaceous aerosols outflow from India and Arabia: Biomass/biofuel burning and fossil fuel combustion, *J. Geophys. Res.*, 108, D15, doi:10.1029/2002JD003277, 2003.
- Gustafsson, Ö., Kruså, M., Zencak, Z., Sheesley, R. J., Granat, L., Engström, E., Praveen, P. S., Rao, P. S. P., Leck, C., and Rodhe, H.: Brown clouds over South Asia: Biomass or fossil fuel combustion?, *Science*, 323, 495–498, doi:10.1126/science.1164857, 2009.
- Hagler, G. S. W., Bergin, M. H., Salmon, L. G., Yu, J. Z., Wan, E. C. H., Zheng, M., Zeng, L. M., Kiang, C. S., Zhang, Y. H., Lau, A. K. H., and Schauer, J. J.: Source areas and chemical composition of fine particulate matter in the Pearl River Delta region of China, *Atmos. Environ.*, 40, 3802–3815, 2006.
- Han, Y. M., Cao, J., Chow, J. C., Watson, J. G., An, Z., Jin, Z., Fung, K., and Liu, S.: Evaluation of the thermal/optical reflectance method for discrimination between char- and soot-EC, *Chemosphere*, 69, 569–574, doi:10.1016/j.chemosphere.2007.03.024, 2007.
- Han, Y. M., Cao, J. J., Posmentier, E. S., Chow, J. C., Watson, J. G., Fung, K. K., Jin, Z. D., Liu, S. X., and An, Z. S.: The effect of acidification on the determination of elemental carbon, char, and soot-elemental carbon in soils and sediments, *Chemosphere*, 75, 92–95, doi:10.1016/j.chemosphere.2008.11.044, 2009a.
- Han, Y. M., Lee, S. C., Cao, J. J., Ho, K. F., and An, Z. S.: Spatial distribution and seasonal variation of char-EC and soot-EC in the atmosphere over China, *Atmos. Environ.*, 43, 6066–6073, doi:10.1016/j.atmosenv.2009.08.018, 2009b.
- Han, Y. M., Cao, J. J., Lee, S. C., Ho, K. F., and An, Z. S.: Different characteristics of char and soot in the atmosphere and their ratio as an indicator for source identification in Xi'an, China, *Atmos. Chem. Phys.*, 10, 595–607, doi:10.5194/acp-10-595-2010, 2010.
- Hansen, A. D. H.: The Aethalometer™, Magee Scientific Company, Berkeley, California, USA, 2005.
- Hansen, J., Sato, M., and Ruedy, R.: Radiative forcing and climate response. *J. Geophys. Res.*, 102, 6831–6864, doi:10.1029/96JD03436, 1997.
- Havers, N., Burba, P., Lambert, J., and Klockow, D.: Spectroscopic characterization of humic-like substances in airborne particulate matter, *J. Atmos. Chem.*, 29, 45–54, doi:10.1023/A:1005875225800, 1998.
- Haywood, J. and Boucher, O.: Estimates of the direct and indirect radiative forcing due to tropospheric aerosols: A review, *Rev. Geophys.*, 38, 513–543, doi:10.1029/1999RG000078, 2000.
- He, K., Yang, F., Ma, Y., Zhang, Q., Yao, X., Chan, C. K., Cadle, S., Chan, T., and Mulawa, P.: The characteristics of PM_{2.5} in Beijing, China, *Atmos. Environ.*, 35, 4959–4970, 2001.
- Hoffer, A., Gelencsér, A., Guyon, P., Kiss, G., Schmid, O., Frank, G. P., Artaxo, P., and Andreae, M. O.: Optical properties of humic-like substances (HULIS) in biomass-burning aerosols, *Atmos. Chem. Phys.*, 6, 3563–3570, doi:10.5194/acp-6-3563-2006, 2006.
- Huebert, B. J., Bates, T., Russell, P. B., Shi, G., Kim, Y. J., Kawamura, K., Carmichael, G., and Nakajima, T.: An overview of ACE-Asia: Strategies for quantifying the relationships between Asian aerosols and their climatic impacts, *J. Geophys. Res.*, 108, 8633, doi:10.1029/2003JD003550, 2003.
- IPCC: Climate Change 2007: The Physical Science Basis (Contribution of Working Group I to the Fourth Assessment Report of the Intergovernmental Panel on Climate Change), edited by: Solomon, S., Qin, D., Manning, M., Chen, Z., Marquis, M., Averyt, K. B., Tignor, M., and Miller, H. L., Cambridge Univ. Press, New York, 131–217, 2007.
- Jacobson, M. Z.: Strong radiative heating due to the mixing state of black carbon in atmospheric aerosols, *Nature*, 409, 695–697, doi:10.1038/35055518, 2001.
- Jacobson, M. C., Hansson, H.-C., Noone, K. J., and Charlson, R. J.: Organic atmospheric aerosols: review and state of the science, *Rev. Geophys.*, 38, 267–294, doi:10.1029/1998RG000045, 2000.
- Jimenez, J. L., Canagaratna, M. R., Donahue, N. M., Prevot, A. S. H., Zhang, Q., Kroll, J. H., DeCarlo, P. F., Allan, J. D., Coe, H., Ng, N. L., Aiken, A. C., Docherty, K. S., Ulbrich, I. M., Grieshop, A. P., Robinson, A. L., Duplissy, J., Smith, J. D., Wilson, K. R., Lanz, V. A., Hueglin, C., Sun, Y. L., Tian, J., Laaksonen, A., Raatikainen, T., Rautiainen, J., Vaattovaara, P., Ehn, M., Kulmala, M., Tomlinson, J. M., Collins, D. R., Cu-

- bison, M. J., E., Dunlea, J., Huffman, J. A., Onasch, T. B., Alfarra, M. R., Williams, P. I., Bower, K., Kondo, Y., Schneider, J., Drewnick, F., Borrmann, S., Weimer, S., Demerjian, K., Salcedo, D., Cottrell, L., Griffin, R., Takami, A., Miyoshi, T., Hatakeyama, S., Shimojo, A., Sun, J. Y., Zhang, Y. M., Dzepina, K., Kimmel, J. R., Sueper, D., Jayne, J. T., Herndon, S. C., Trimborn, A. M., Williams, L. R., Wood, E. C., Middlebrook, A. M., Kolb, C. E., Baltensperger, U., and Worsnop, D. R.: Evolution of Organic Aerosols in the Atmosphere, *Science*, 326, 1525, doi:10.1126/science.1180353, 2009.
- Kanakidou, M., Seinfeld, J. H., Pandis, S. N., Barnes, I., Dentener, F. J., Facchini, M. C., Van Dingenen, R., Ervens, B., Nenes, A., Nielsen, C. J., Swietlicki, E., Putaud, J. P., Balkanski, Y., Fuzzi, S., Horth, J., Moortgat, G. K., Winterhalter, R., Myhre, C. E. L., Tsigaridis, K., Vignati, E., Stephanou, E. G., and Wilson, J.: Organic aerosol and global climate modelling: a review, *Atmos. Chem. Phys.*, 5, 1053–1123, doi:10.5194/acp-5-1053-2005, 2005.
- Kim, Y. P., Moon, K.-C., and Lee, J. H.: Organic and elemental carbon in fine particles at Kosan, Korea, *Atmos. Environ.*, 34, 3309–3317, 2000.
- Kim, S.-W., Yoon, S.-C., Kim, J., and Kim, S.-Y.: Seasonal and monthly variations of columnar aerosol optical properties over east Asia determined from multi-year MODIS, LIDAR, and AERONET Sun/sky radiometer measurements, *Atmos. Environ.*, 41, 1634–1651, doi:10.1016/j.atmosenv.2006.10.044, 2007.
- Kirchstetter, T. W., Novakov, T., and Hobbs, P. V.: Evidence that the spectral dependence of light absorption by aerosols is affected by organic carbon, *J. Geophys. Res.*, 109, D21208, doi:10.1029/2004JD004999, 2004.
- Koçak, M., Mihalopoulos, N., and Kubilay, N.: Chemical composition of the fine and coarse fraction of aerosols in the Northeastern Mediterranean, *Atmos. Environ.*, 41, 7351–7368, 2007.
- Kuhlbusch, T. A. J.: Black carbon in soils, sediments, and ice cores, in: *Environmental analysis and remediation*, edited by: Meyers, R. A., John Wiley & Sons, Toronto, Canada, 813–823, 1997.
- Lee, M., Song, M., Moon, K. J., Han, J. S., Lee, G., and Kim, K.-R.: Origins and chemical characteristics of fine aerosols during the northeastern Asia regional experiment (Atmospheric Brown Cloud – East Asia Regional Experiment 2005), *J. Geophys. Res.*, 112, D22S29, doi:10.1029/2006JD008210, 2007.
- Lee, J. Y., Kim, Y. P., Bae, G. N., Park, S. M., and Jin, H. C.: The characteristics of particulate PAHs concentrations at a roadside in Seoul, *Korean J. Atmos. Environ.*, 24, 133–142, 2008.
- Lee, H. W., Lee, T. J., and Kim, D. S.: Identifying Ambient PM_{2.5} Sources and estimating their contributions by using PMF: Separation of gasoline and diesel automobile sources by analyzing ECs and OCs, *J. Korean Soc. Atmos. Environ.*, 25, 75–89, 2009.
- Li, X., Shen, Z., Cao, J., Liu, S., Zuh, C., and Zhang, T.: Distribution of carbonaceous aerosol during spring 2005 over the Horquin sandland in northeastern China, *China Particology*, 4, 316–322, doi:10.1016/S1672-2515(07)60282-6, 2006.
- Lim, S.: Source Signature of Ions and Carbonaceous Compounds in Submicron and Supermicron Aerosols at Gosan-super site, Jeju, South Korea, Master's thesis, Korea University, 2009.
- Lim, S., Lee, M., and Kang, K.: Seasonal Variations of OC and EC in PM₁₀, PM_{2.5} and PM_{1.0} at Gosan Superstation on Jeju Island, *Korean J. Atmos. Environ.*, 26, 567–580, 2010a.
- Lim, S., Lee, M., Lee, G., and Kang, K.: Source signature of mass, nitrate and sulfate in supermicron and submicron aerosols at Gosan Superstation on Jeju Island, *J. Atmos.*, 20, 221–228, 2010b.
- Lin, C.-Y., Wang, Z., Chen, W.-N., Chang, S.-Y., Chou, C. C. K., Sugimoto, N., and Zhao, X.: Long-range transport of Asian dust and air pollutants to Taiwan: observed evidence and model simulation, *Atmos. Chem. Phys.*, 7, 423–434, doi:10.5194/acp-7-423-2007, 2007.
- Liu, X., Zhang, W., Wang, Z., Zhao, W., Tao, L., and Yang, X.: Chemical composition and size distribution of secondary organic aerosol formed from the photooxidation of isoprene, *J. Environ. Sci.*, 21, 1525–1531, 2009.
- Mace, K. A., Kubilay, N., and Duce, R. A.: Organic nitrogen in rain and aerosol in the eastern Mediterranean: an association with atmospheric dust, *J. Geophys. Res.*, 108, 4320–4330, doi:10.1029/2002JD002997, 2003.
- Mamane, Y. and Gottlieb, J.: Heterogeneous reactions of minerals with sulfur and nitrogen oxides, *J. Aerosol Sci.*, 20, 303–311, doi:10.1016/0021-8502(89)90006-2, 1989.
- Maria, S. F., Russell, L. M., Gilles, M. K., and Myrneni, S. C. B.: Organic aerosol growth mechanisms and their climate-forcing implications, *Science*, 306, 1921–1924, doi:10.1126/science.1103491, 2004.
- Martins, J. V., Artaxo, P., Liousse, C., Reid, J. S., Hobbs, P. V., and Kaufman, Y. J.: Effects of black carbon content, particle size, and mixing on light absorption by aerosols from biomass burning in Brazil, *J. Geophys. Res.*, 103, 32041–32050, 1998.
- Masiello, C. A.: New directions in black carbon organic geochemistry, *Mar. Chem.*, 92, 201–213, 2004.
- Mochida, M., Umemoto, N., Kawamura, K., Lim, H.-J., and Turpin, B. J.: Bimodal size distributions of various organic acids and fatty acids in the marine atmosphere: Influence of anthropogenic aerosols, Asian dusts, and sea spray off the coast of East Asia, *J. Geophys. Res.*, 112, D15209, doi:10.1029/2006JD007773, 2007.
- Moon, K. J., Han, J. S., Ghim, Y. S., and Kim, Y. J.: Source apportionment of fine carbonaceous particles by positive matrix factorization at Gosan background site in East Asia, *Environ. Int.*, 34, 654–664, 2008.
- Mukai, H. and Ambe, Y.: Characterization of a humic acid-like brown substance in airborne particulate matter and tentative identification of its origin, *Atmos. Environ.*, 20, 813–819, 1986.
- Novakov, T. and Corrigan, C. E.: Thermal characterization of biomass smoke particles, *Mikrochim. Acta*, 119, 157–166, 1995.
- Nunes, T. V. and Pio, C. A.: Carbonaceous aerosols in industrial and coastal atmosphere, *Atmos. Environ.*, 27, 1339–1346, 1993.
- Ogren, J. A. and Charlson, R. J.: Elemental carbon in the atmosphere: cycle and lifetime, *Tellus Series B-Chemical and Physical Meteorology*, 35B, 241–254, doi:10.1111/j.1600-0889.1983.tb00027.x, 1983.
- Ohta, S., Hori, M., Yamagata, S., and Murao, N.: Chemical characterization of atmospheric fine particles in Sapporo with determination of water content, *Atmos. Environ.*, 32, 1021–1025, 1998.
- Park, S. S., Kim, Y. J., and Fung, K.: Characteristics of PM_{2.5} carbonaceous aerosol in the Sihwa industrial area, Korea, *Atmos. Environ.*, 35, 657–665, 2001.
- Park, R., Kim, M., Jeong, J., Youn, D., and Kim, S.: A contribution of brown carbon aerosol to the aerosol light absorption and its radiative forcing in East Asia, *Atmos. Environ.*, 44, 1414–1421, doi:10.1016/j.atmosenv.2010.01.042, 2010.

- Persiantseva, N. M., Popovicheva, O. B., and Shonija, N. K.: Wet-ting and hydration of insoluble soot particles in the upper troposphere, *J. Environ. Monit.*, 6, 939–945, 2004.
- Petzold, A., Gysel, M., Vancassel, X., Hitzengerger, R., Puxbaum, H., Vrochticky, S., Weingartner, E., Baltensperger, U., and Mirabel, P.: On the effects of organic matter and sulphur-containing compounds on the CCN activation of combustion particles, *Atmos. Chem. Phys.*, 5, 3187–3203, doi:10.5194/acp-5-3187-2005, 2005.
- Pey, J., Pérez, N., Castillo, S., Viana, M., Moreno, T., Pandolfi, M., López-Sebastián, J.M., Alastuey, A., and Querol, X.: Geochemistry of regional background aerosols in the Western Mediterranean, *Atmos. Res.*, 94, 422–435, 2009.
- Qu, W. J., Zhang, X. Y., Arimoto, R., Wang, Y. Q., Wang, D., Sheng, L. F., and Fu, G.: Aerosol background at two remote CAWNET sites in western China, *Sci. Total Environ.*, 407, 3518–3529, 2009.
- Ramachandran, S., Rengarajan, R., and Sarin, M. M.: Atmospheric carbonaceous aerosols: issues, radiative forcing and climate impacts, *Cur. Sci. Com.*, 97, 18–20, 2009.
- Ramana, M. V., Ramanathan, V., Feng, Y., Yoon, S.-C., Kim, S.-W., and Carmichael, G. R.: Warming influenced by the ratio of black carbon to sulphate and the black-carbon source, *Nature Geosci.*, 3, 542–545, doi:10.1038/NCEO918, 2010.
- Ramanathan, V. and Carmichael, G.: Global and regional climate changes due to black carbon, *Nature Geosci.*, 1, doi:10.1038/ngeo156, 2008.
- Ramanathan, V. and Xu, Y.: The Copenhagen Accord for limiting global warming: Criteria, constraints, and available avenues, *PNAS*, 107, 8055–8062, doi:10.1073/pnas.1002293107, 2010.
- Ramanathan, V., Crutzen, P. J., Kiehl, J. T., and Rosenfeld, D.: Atmosphere – Aerosols, climate, and the hydrological cycle, *Science*, 294, 2119–2124, doi:10.1126/science.1064034, 2001.
- Ravishankara, A. R.: Heterogeneous and multiphase chemistry in the Troposphere, *Science*, 276, 1058–1065, doi:10.1126/science.276.5315.1058, 1997.
- Robertson, A., Overpeck, J., Rind, D., Mosley-Thompson, E., Zielinski, G., Lean, J., Koch, D., Penner, J., Tegen, I., and Healy, R.: Hypothesized climate forcing time series for the last 500 years, *J. Geophys. Res.*, 106, 14783–14803, doi:10.1029/2000JD900469, 2001.
- Russell, L. M., Maria, S. F., and Myneni, S. C. B.: Mapping organic coatings on atmospheric particles, *Geophys. Res. Lett.*, 29, 1779, doi:10.1029/2002GL014874, 2002.
- Schnaiter, M., Horvath, H., Mohler, O., Naumann, K.-H., Saathoff, H., and Schock, O. W.: UV-VIS-NIR spectral optical properties of soot and soot-containing aerosols, *J. Aerosol Sci.*, 34, 1421–1444, doi:10.1016/S0021-8502(03)00361-6, 2003.
- Shah, J. J., Johnson, R. L., Heyerdahl, E. K., and Huntzicker, J. J.: Carbonaceous aerosol at urban and rural sites in the United States, *J. Air Pollut. Control Assoc.*, 36, 254–257, 1986.
- Shen, Z. X., Cao, J. J., Arimoto, R., Zhang, R. J., Jie, D. M., Liu, S. X., and Zhu, C. S.: Chemical composition and source characterization of spring aerosol over Horqin sand land in northeastern China, *J. Geophys. Res.*, 112, D14315, doi:10.1029/2006JD007991, 2007.
- Silva, P. J., Liu, D. Y., Noble, C. A., and Prather, K. A.: Size and chemical characterization of individual particles resulting from biomass burning of local southern California species, *Environ. Sci. Technol.*, 33, 3068, doi:10.1021/es980544p, 1999.
- Stohl, A., Forster, C., Frank, A., Seibert, P., and Wotawa, G.: Technical note: The Lagrangian particle dispersion model FLEXPART version 6.2, *Atmos. Chem. Phys.*, 5, 2461–2474, doi:10.5194/acp-5-2461-2005, 2005.
- Streets, D. G., Bond, T. C., Carmichael, G. R., Fernandes, S. D., Fu, Q., He, D., Klimont, Z., Nelson, S. M., Tsai, N. Y., Wang, M. Q., Woo, J.-H., and Yarber, K. F.: An inventory of gaseous and primary aerosol emissions in Asia in the year 2000, *J. Geophys. Res.*, 108, GTE30-1-GTE30-23, doi:10.1029/2002JD003093, 2003.
- Szidat, S., Ruff, M., Perron, N., Wacker, L., Synal, H.-A., Hallquist, M., Shannigrahi, A. S., Yttri, K. E., Dye, C., and Simpson, D.: Fossil and non-fossil sources of organic carbon (OC) and elemental carbon (EC) in Göteborg, Sweden, *Atmos. Chem. Phys.*, 9, 1521–1535, doi:10.5194/acp-9-1521-2009, 2009.
- Talbot, R. W., Harriss, P. C., Browell, E. V., Gregory, G. L., Sebacher, D. I., Beck, S. M.: Distribution and geochemistry of aerosols in the tropical north Atlantic troposphere: relationship to Saharan dust, *J. Geophys. Res.*, 91, 5173–5182, doi:10.1029/JD091iD04p05173, 1986.
- Tsigaridis, K., Krol, M., Dentener, F. J., Balkanski, Y., Lathière, J., Metzger, S., Hauglustaine, D. A., and Kanakidou, M.: Change in global aerosol composition since preindustrial times, *Atmos. Chem. Phys.*, 6, 5143–5162, doi:10.5194/acp-6-5143-2006, 2006.
- Wang, Y., Zhuang, G., Tang, A., Zhang, W., Sun, Y., Wang, Z., and An, Z.: The evolution of chemical components of aerosols at five monitoring sites of China during dust storms, *Atmos. Environ.*, 41, 1091–1106, 2007.
- Worsnop, D. R., Morris, J. W., Shi, Q., Davidovits, P., and Kolb, C. E.: A chemical kinetic model for reactive transformations of aerosol particles, *Geophys. Res. Lett.*, 29, 57-1–57-4, doi:10.1029/2002GL015542, 2002.
- Wu, P. M. and Okada, K.: Nature of coarse nitrate particles in the atmosphere: a single particle approach, *Atmos. Environ.*, 28, 2053–2060, 1994.
- Yang, F., He, K., Ye, B., Chen, X., Cha, L., Cadle, S. H., Chan, T., and Mulawa, P. A.: One-year record of organic and elemental carbon in fine particles in downtown Beijing and Shanghai, *Atmos. Chem. Phys.*, 5, 1449–1457, doi:10.5194/acp-5-1449-2005, 2005.
- Ye, B., Ji, X., Yang, H., Yao, X., Chan, C. K., Cadle, S. H., Chan T., Mulawa, P. A.: Concentration and chemical composition of PM_{2.5} in Shanghai for a 1-year period, *Atmos. Environ.*, 37, 499–510, 2003.
- Zhang, Y., Sunwoo, Y., Kotamarthi, V., and Carmichael, G. R.: Photochemical oxidant processes in the presence of dust: an evaluation of the impact of dust on particulate nitrate and ozone formation, *J. Applied Meteorology*, 33, 7, 813–824, doi:10.1175/1520-0450(1994)033<0813:POPITP>2.0.CO;2, 1994.
- Zhang, R., Cao, J., Lee, S., Shen, Z., and Ho, K.: Carbonaceous aerosols in PM₁₀ and pollution gases in winter in Beijing, *J. Environ. Sci.*, 19, 564–571, 2007.